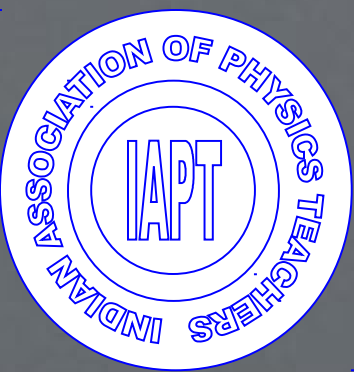


Vol 32 No. 3 Jul - Sep 2016 ISSN 0970-5953



PHYSICS EDUCATION



First time that India (ISRO) has deployed satellites in two different orbits during a single launch, lunched on Monday 27 Sep. 2016.

www.physedu.in

Volume 32, Number 3**In this Issue**

- **Editorial** 01 page
M. S. Santhanam
- **How Large Is An Atom?** 07 pages
M. N. Murty
- **Evaluation of Boltzmann’s constant: Revisit using interfaced data analysis.** 05 pages
S. V.Luthra, A. Kaur, S.Saini, S. Jaglan, S. Dhasmana, Apoorva and Ajith B.P.
- **Magnetic Actuators in order to study Faraday Force** 08 pages
Takuo Sakon, Seiji Nitabaru, Takahiro Higasa, Yasushi Hara and Keisuke Nakagawa
- **Gibbs paradox: Mixing and non mixing potentials** 10 pages
T. P. Suresh , Lisha Damodaran and K. M. Udayanandan
- **Using an iPad to Learn Motion Concepts in Introductory Physics** 11 pages
Tarlok S. Aurora
- **Teaching Special Relativity with Real Rotation Matrix** 04 pages
E. Benedetto
- **Book Review: Quantum Field Theory The Why, What and How - Thanu PADMANABHAN** 05 Pages
R Ramachandran

EDITORIAL

This issue of Physics Education comes to you with the cover page sporting a rocket launch. Last week, the Indian Space Research Organization (ISRO) launched satellites in two different orbits from a single PSLV rocket. This month ISRO launched GSLV rocket that can successfully put 2000 kg class artificial satellites in geosynchronous orbits. In June this year, ISRO launched 22 satellites from a single launch. It has been a successful year for ISRO. Around the world, these are exciting times as well for space flight ventures. The privately held US based company SpaceX is attempting smooth landing of rockets back on earth for reusing them. It has also set the sights on making travel to Mars a routine exercise.

While on Many decades back, Vikram Sarabhai, the pioneer of India's space program, had clearly spelt out the need for India to join the space explorers club, not for elusive status tag it offers

but for societal benefits. He said, “There are some who question the relevance of space activities in a developing nation. To us, there is no ambiguity of purpose. We do not have the fantasy of competing with the economically advanced nations in the exploration of the moon or the planets or manned space-flight. But we are convinced that if we are to play a meaningful role nationally, and in the community of nations, we must be second to none in the application of advanced technologies to the real problems of man and society“. ISRO has not only fulfilled his vision of contributing to India's requirements, but has gone beyond to explore the moon and the Mars.

M. S. Santhanam
Chief Editor
Physics Education

How Large Is An Atom?

M. N. Murty

Visiting Faculty, Department of Physics,
Sri Sathya Sai Institute of Higher Learning,
Prasanthi Nilayam – 515134, Andhra Pradesh, India.

E-mail: mnarayanamurty@rediffmail.com

(Submitted: 10-03-2016)

Abstract

The atomic radius of a chemical element is a measure of the size of its atoms. Atomic radii represent the sizes of isolated and electrically neutral atoms. In this paper, simple calculations for radii of hydrogen, helium and neon are given. Victor Weisskopf has calculated the radii of different atoms. To calculate the potential energy of electrons due to mutual repulsion among them, Weisskopf has assumed that the effective distance r_{eff} between two electrons is $r/0.6$, where r is the radius of the orbit of electrons. There is a good agreement between the calculated values and the experimentally measured values of the radii of atoms. The atomic radii gradually decrease along each period of the periodic table, from the alkali metals to the noble gases; and increase down each group. The radii of isolated neutral atoms range between 0.3 and 3 angstroms. The radius of an atom is a function of its environment.

1. Introduction

Victor Weisskopf has calculated the radii of different atoms. To calculate the potential energy of electrons due to mutual repulsion among them, Weisskopf has assumed that the effective distance r_{eff} between two electrons is $r/0.6$, where r is the radius of the orbit of electrons. The atomic radius of a chemical element is a measure of the size of its atoms. Atomic radii represent the sizes of isolated and electrically neutral atoms.

The rest of the paper is organised as follows. The sizes of the hydrogen atom, helium atom and neon atom are given in Section 2, Section 3 and Section 4 respectively. General discussion on atomic size is presented in Section 5. Conclusions are given in Section 6.

2. The size of hydrogen atom

According to Bohr, electrons go round the nucleus in certain circular orbits, known as Bohr orbits. The velocity v of the electron in a circular orbit of radius r satisfies the quantization condition

$$m_e v r = n \hbar \quad (1)$$

where, m_e the mass of the electron is 9.1×10^{-31} Kg.

$\hbar = h/2\pi$, $h =$ Planck's constant = 6.62×10^{-34} J-s

$n =$ No. of the orbit of the electron = 1, 2, 3,

n is known as *principal quantum number*. According to (1), the angular momentum of an electron revolving around the nucleus in a circular orbit is an integral multiple of \hbar . Only those circular orbits for which (1) is true are allowed.

Let us find out the radius of first Bohr orbit of hydrogen atom. The kinetic energy K of electron revolving around the proton in hydrogen atom is given by

$$K = \frac{p^2}{2m} \quad (2)$$

where $p = m_e v$ = the momentum of the electron. Electrons can behave both as particles and waves, known as de Broglie waves. According to de Broglie, the electron wavelength λ is given by

$$\lambda = h/p \quad (3)$$

Using (3) in (1), we have for first orbit ($n = 1$)

$$r = \frac{h}{m_e v} = \frac{h}{2\pi p} = \frac{\lambda}{2\pi} \\ \Rightarrow \lambda = 2\pi r \quad (4)$$

This equation shows that one electron wave is wrapped around the first orbit. Substituting (3) and (4) in (2), we get

$$K = \frac{h^2}{2m_e \lambda^2} = \frac{h^2}{2m_e r^2} \quad (5)$$

The potential energy V of the electron is due to electrostatic interaction and gravitational interaction between itself and the proton.

The gravitational potential energy of the electron = $V_g = -\frac{Gm_p m_e}{r}$

The electrostatic potential energy of the electron = $V_e = -\frac{e^2}{4\pi\epsilon_0 r}$

Where, G = gravitational constant = $6.67 \times 10^{-11} \text{m}^3/\text{Kg}\cdot\text{S}^2$

m_p = mass of a proton = $1.67 \times 10^{-27} \text{Kg}$

ϵ = permittivity of free space = $8.85 \times 10^{-12} \text{F/m}$

e = charge of an electron = $1.6 \times 10^{-19} \text{C}$.

Now the ratio

$$\frac{V_g}{V_e} = \frac{4\pi\epsilon_0 G m_p m_e}{e^2} \approx \frac{1}{2.27 \times 10^{39}}$$

This value shows that the gravitational attraction between proton and electron in

hydrogen atom is very much weaker than electrostatic attraction. Hence the gravitational potential V_g can be neglected in comparison with electrostatic potential. The V_g in the potential energy V of the electron is given by

$$V \approx V_e = -\frac{e^2}{4\pi\epsilon_0 r} \quad (6)$$

The total energy E of the electron is obtained by adding (5) and (6).

$$E = K + V = \frac{h^2}{2m_e r^2} - \frac{e^2}{4\pi\epsilon_0 r} \quad (7)$$

To find the value of r , when E is minimum, we must set the derivative $\frac{dE}{dr}$ equal to zero.

$$\frac{dE}{dr} = -\frac{h^2}{m_e r^3} + \frac{e^2}{4\pi\epsilon_0 r^2} = 0 \\ \Rightarrow r = 4\pi\epsilon_0 \frac{h^2}{m_e e^2}$$

This particular value of r when E is minimum is denoted by a_0 , known as *Bohr radius*.

$$\therefore a_0 = 4\pi\epsilon_0 \frac{h^2}{m_e e^2} \\ = 0.528 \times 10^{-10} \text{m} = 0.528 \text{\AA} \quad (8)$$

The state of the hydrogen atom corresponding to the orbit with radius equal to *Bohr radius* a_0 is called the *ground state*.

Now let us consider the case where the electron is in the second Bohr orbit. Since the energy of this state is higher, it is known as *first excited state*. From (1), we have for the first excited state ($n = 2$)

$$m_e v r = 2\hbar \\ \Rightarrow r = 2 \frac{h}{m_e v} = 2 \left(\frac{h}{2\pi p} \right)$$

Using (3) in the above expression, we obtain

$$2\pi r = 2\lambda \quad (9)$$

This equation shows that two wavelengths would be wrapped around the second orbit. Using (9), the kinetic energy of the electron in the second orbit is given by

$$K = \frac{h^2}{2m_e \lambda^2} = 4 \left(\frac{\hbar^2}{2m_e r^2} \right) \quad (10)$$

The potential energy of the electron in the second orbit is given by same equation (6). The energy E of the electron in the second orbit is obtained by adding (6) and (10).

$$E = 4 \left(\frac{\hbar^2}{2m_e r^2} \right) - \frac{e^2}{4\pi\epsilon_0 r} \quad \text{Equating}$$

$\frac{dE}{dr}$ to zero, we get

$$r_1 = 4 \left[4\pi\epsilon_0 \left(\frac{\hbar^2}{m_e e^2} \right) \right] \quad (11)$$

Where, r_1 = radius of second orbit

Using (8) in (11), we get

$$r_1 = 4a_0 = 2^2 a_0 \quad (12)$$

This expression shows that the radius of second orbit is four times the radius of first orbit. So, in general the radius of n th orbit of hydrogen atom is $n^2 a_0$.

3. The size of helium atom

There are two electrons in the helium atom and its nucleus consists of two protons and two neutrons. In the ground state both these electrons rotate in the same orbit around the nucleus.

Using (5) the kinetic energy K of two electrons in helium is given by

$$K = 2 \left(\frac{\hbar^2}{2m_e r^2} \right) \quad (13)$$

The potential energy of the two electrons due to the electrostatic attraction of the nucleus having the charge $+2e$ is

$$V_1 = 2 \left(-\frac{2e^2}{4\pi\epsilon_0 r} \right) = -4 \left(\frac{e^2}{4\pi\epsilon_0 r} \right) \quad (14)$$

To calculate the net potential energy of two electrons, we have to take into account the electrostatic repulsion between the electrons also. The minimum distance between the two electrons is zero (Figure 1a), but that would lead to infinite energy, which is unacceptable. The maximum possible distance between the two electrons is $2r$ (Figure 1b).

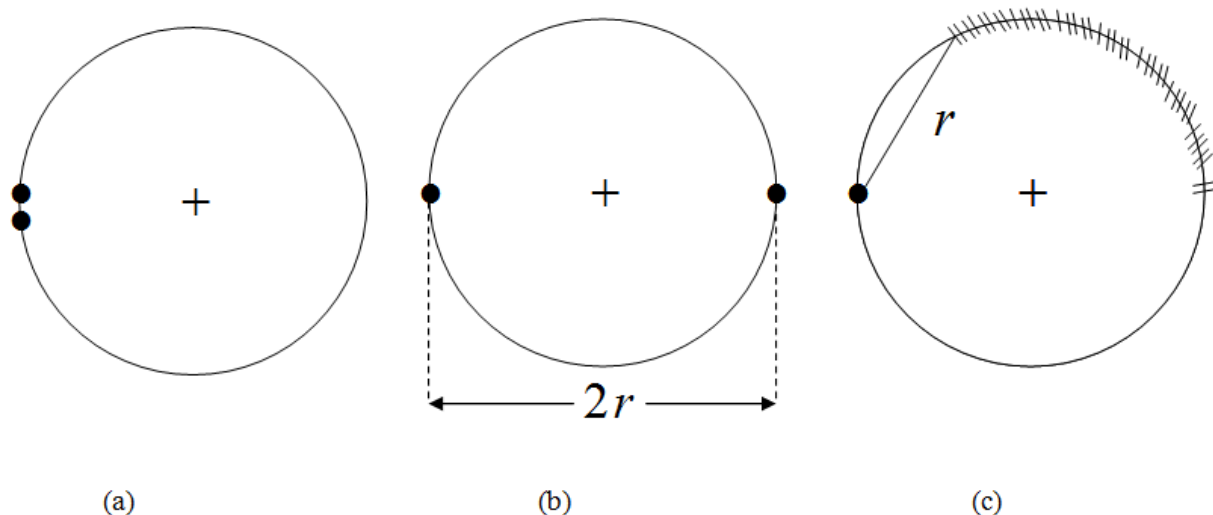


Figure1. Two electrons in the lowest orbit of helium (a) shows a case which is ruled out because of infinite repulsion energy (b) shows the maximum distance between two electrons (c) shows that the second electron is somewhere in the shaded region according to Weisskopf.

According to Weisskopf, the two electrons on the average are at a distance r_{eff} apart (Figure 1c), such that

$$r < r_{eff} < 2r \quad (15)$$

Weisskopf has assumed that the effective distance r_{eff} between two electrons is $r/0.6$.

$$r_{eff} = \frac{r}{0.6} \quad (16)$$

Hence, the potential energy of the two electrons due to electrostatic repulsion between them is given by

$$V_2 = \frac{1}{4\pi\epsilon_0} \left(\frac{e^2}{r_{eff}} \right)$$

Substituting (16) in the above expression, we get

$$V_2 = \frac{0.6}{4\pi\epsilon_0} \left(\frac{e^2}{r} \right) \quad (17)$$

Addition of (14) and (17) gives the net potential energy V of two electrons.

$$V = V_1 + V_2 = (-4 + 0.6) \frac{e^2}{4\pi\epsilon_0 r}$$

$$\Rightarrow V = (-3.4) \frac{e^2}{4\pi\epsilon_0 r} \quad (18)$$

The total energy E of two electrons is found out by adding (13) and (18).

$$E = 2 \left(\frac{\hbar^2}{2m_e r^2} \right) - (3.4) \frac{e^2}{4\pi\epsilon_0 r} \quad (19)$$

Equating $\frac{dE}{dr}$ to zero, the radius of the orbit

of two electrons of helium atom in the ground state is given by

$$r = \frac{2}{3.4} \left(4\pi\epsilon_0 \frac{\hbar^2}{m_e e^2} \right)$$

Using (8) for *Bohr radius* in the above expression, we have

$$r \approx 0.588a_0 \approx 0.6a_0 \quad (20)$$

4. The size of neon atom

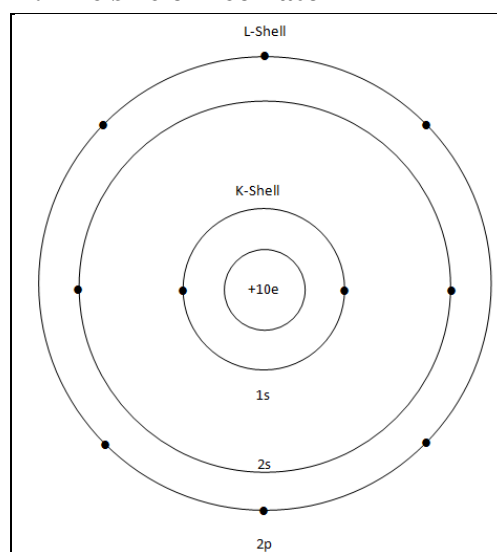


Figure 2.Arrangement of electrons in neon atom.

Neon atom has 10 electrons. These electrons are present in two shells, K-shell and L-shell. K-shell has one sub shell, 1s, and L-shell has two sub shells, 2s and 2p. The electronic configuration of Ne atom is $1s^2, 2s^2, 2p^6$. The arrangement of electrons in neon atom is shown in Figure 2.

Weisskopf has calculated the radius of L-shell. The electrons in L-shell see the nucleus which has a charge $+10e$ and also they see the two electrons in K-shell. So,

the net charge seen by electrons of L-shell is $+10e - 2e = +8e$. The radius L-shell is calculated by taking the effective nuclear charge as $Z_{eff} = +8e$.

The kinetic energy K of electrons in the L-shell is calculated by taking it as the second orbit of hydrogen atom. As per (10), the contribution of each electron in L-shell to kinetic energy is $4\hbar^2/2m_e r^2$. Since L-shell contains 8 electrons, we have

$$K = 8 \times \left(\frac{4\hbar^2}{2m_e r^2} \right) = 32 \left(\frac{\hbar^2}{2m_e r^2} \right) \quad (21)$$

The potential energy of 8 electrons in L-shell is calculated by taking into account the electrostatic attraction on these electrons by the nucleus with effective charge +8e as well as the repulsive forces among these electrons.

The potential energy of 8 electrons in L-shell due to electrostatic attraction of nucleus having effective charge +8e is given by

$$V_1 = 8 \times \left(-\frac{8e^2}{4\pi\epsilon_0 r} \right) \quad (22)$$

The 8 electrons in L-shell are formed into pairs to calculate the potential energy due to repulsive forces among them. The 8 electrons can be formed into $\frac{8 \times 7}{2} = 28$ distinct pairs. As in helium atom, the effective distance r_{eff} between two electrons of a pair is taken as $r/0.6$. Since there are 28 pairs of electrons, the potential energy of electrons in L-shell due to repulsive forces among them is given by

$$\begin{aligned} V_2 &= 28 \times \left(\frac{e^2}{4\pi\epsilon_0 r_{eff}} \right) \\ &= 28 \times 0.6 \left(\frac{e^2}{4\pi\epsilon_0 r} \right) \end{aligned} \quad (23)$$

The total potential energy V of electrons in L-shell is found out by adding (22) and (23),

$$\begin{aligned} V &= V_1 + V_2 = (-8^2 + 28 \times 0.6) \frac{e^2}{4\pi\epsilon_0 r} \\ \Rightarrow V &= -47.2 \times \frac{e^2}{4\pi\epsilon_0 r} \approx -47 \left(\frac{e^2}{4\pi\epsilon_0 r} \right) \end{aligned} \quad (24)$$

Addition of (21) and (24) gives the total energy E of electrons in L-shell.

$$E = 32 \left(\frac{\hbar^2}{2m_e r^2} \right) - 47 \left(\frac{e^2}{4\pi\epsilon_0 r} \right)$$

Equating $\frac{dE}{dr}$ to zero, the radius of the orbit of electrons in L-shell of neon atom in the ground state is given by

$$r = \frac{32}{47} \left(4\pi\epsilon_0 \frac{\hbar^2}{m_e e^2} \right)$$

Using (8) in the above expression, we get

$$r = \frac{32}{47} a_0 \approx 0.7 a_0 \quad (25)$$

Similar calculations can be made for other atoms using very simple physical arguments. In all cases, the effective distance between any two electrons r_{eff} in any orbit of radius r is taken as $r/0.6$. There is good agreement between the calculated value of radius of an orbit of an atom and the experimental value.

In general the radius of n th shell is given by

$$r = \frac{n^2}{Z_{eff} - (Z_{eff} - 1) \times 0.3} \quad (26)$$

Where, Z_{eff} = effective atomic number of the atom

5. General discussion on atomic size

Table 1 compares the calculated values of atomic radii with the measured values for the first ten elements. There is a good agreement between the calculated values and the experimentally measured values of the radii of atoms.

Table1. Atomic radii of first ten elements

Element	Z	Z_{eff}	n	r in units of a_0 (calculated)	r in units of a_0 (measured)
H	1	1	1	1.0	1.0
He	2	2	1	0.6	0.6
Li	3	1	2	4.0	2.8

Be	4	2	2	2.4	2.2
B	5	3	2	1.7	1.6
C	6	4	2	1.3	1.2
N	7	5	2	1.1	1.0
O	8	6	2	0.9	0.8
F	9	7	2	0.8	0.7
Ne	10	8	2	0.7	0.6

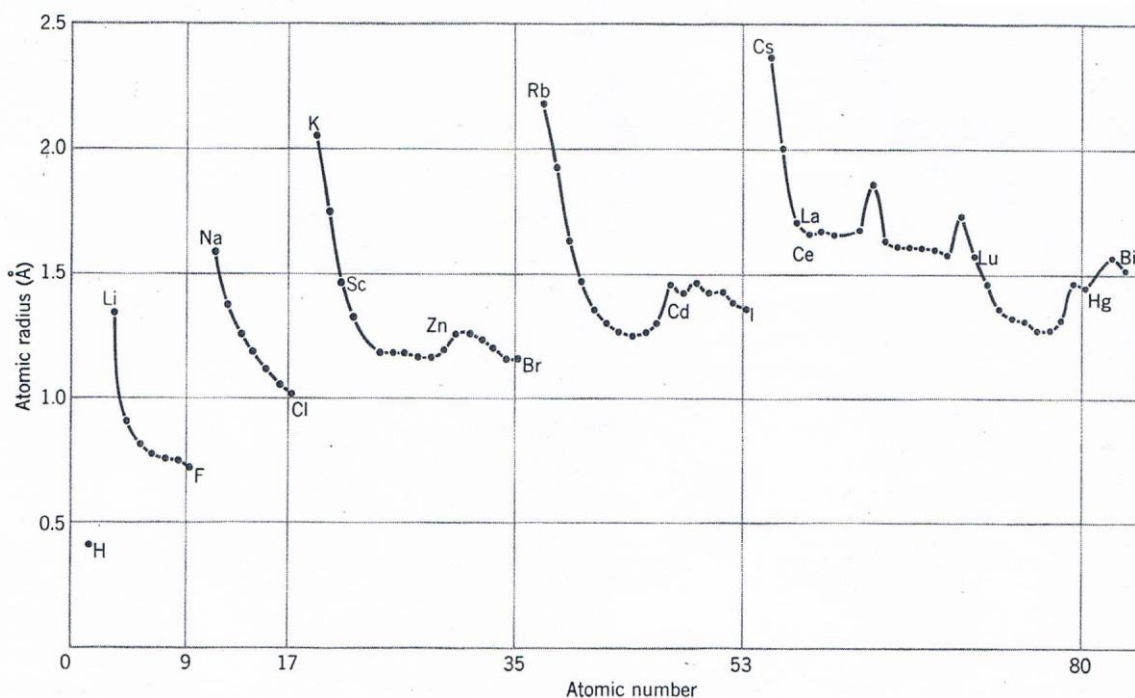


Figure 3. Variation of atomic radius with atomic number.

The variation of atomic radius or atomic size with atomic number for the elements is shown in Figure 3. The following general conclusions can be drawn from this plot.

1. The alkali elements Li, Na, . . . etc., have large radii.
2. Following each alkali element, there is a progressive decrease in atomic radii from left to right along a period in the periodic table.
3. The atomic radius increases sharply between the noble gas at the end of each period and the alkali metal at the beginning of the next period.

4. As we proceed down each group of the periodic table, the atomic radius gradually increases.
5. The variation in atomic size across a period is not always a smooth one, as irregularities are occurring in period 6.

Within a given period, the atomic radius decreases with increasing atomic number owing to the effect of increasing the positive nuclear charge while adding electrons to the same level. Therefore, the effective nuclear charge towards the outermost electrons increases, drawing the outermost electrons closer. As a result, the electrons cloud contracts and the atomic

radius decreases. In a noble gas, the outermost shell is completely filled. Therefore, the addition of electron of next alkali metal will go into a new outer shell, accounting for the sudden increase in the atomic radius.

Within a given group, the atomic radius increases with atomic number because of addition of another level. As we proceed downward from one atom to another within a group, each successive element has its outer electrons in a shell with larger value of n . The effective nuclear charge felt by these electrons stays nearly the same, so the dominant effect is an increase in size of the atom that accompanies an increase in the value of the principal quantum number of the outer-shell orbital.

The radii of isolated neutral atoms range between 0.3 and 3 angstroms. Caesium is the largest known atom. The atomic radius of Cs is given variously as 273.1pm, 265pm, 265.5pm or 260pm ($1\text{pm} = 1 \times 10^{-12}\text{m}$). Caesium has a large valence shell and relatively low effective nuclear charge. A low nuclear charge means that

electrons can wander further, on average, from the nucleus. Rubidium also has large atoms, but its atomic radius is almost 30pm less than that of caesium.

The radius of an atom is a function of its environment. An example is the hydrogen atom, which is assigned with one radius when it combines with itself, a second radius when it combines with the elements of the second period, a third radius when it combines with the elements of the third period, and so on.

6. Conclusion

Victor Weisskopf has calculated the radii of different atoms. The atomic radius of a chemical element is a measure of the size of its atoms. There is a good agreement between the calculated values and the experimentally measured values of the radii of atoms. The atomic radii gradually decrease along each period of the periodic table, from the alkali metals to the noble gases; and increase down each group. The radii of isolated neutral atoms range between 0.3 and 3 angstroms. The radius of an atom is a function of its environment. *and Structure*, (John Wiley & Sons, 1986).

[5] Frank Brescia, John Arents, Herbert Meislich and Amos Turk, *Fundamentals of Chemistry*, (Academic Press, Inc., 1966).

[6] Richard P Feynman, Robert B Leighton and Matthew Sands, *The Feynman Lectures on Physics - Quantum Mechanics*, Vol.III, (Addison-Wesley Publishing Company, Inc., 1963).

References

- [1] G Venkataraman, *Why Are Things the Way They Are?*, (Universities Press, 1992).
- [2] Victor F. Weisskopf, *Am. J. Phys.* 53(3), 206-207 (1985).
- [3] Victor F. Weisskopf, *Am. J. Phys.* 53(4), 304-305 (1985).
- [4] James E Brady and Gerard E Humiston, *General Chemistry Principles*

Evaluation of Boltzmann's constant: Revisit using interfaced data analysis

V.Luthra^{1#}, A. Kaur², S.Saini³, S. Jaglan¹, S.Dhasmana¹, Apoorva¹ and Ajith B.P.⁴

¹Department of Physics
Gargi College
Siri Fort Road,
New Delhi-110049, India

²Department of Mathematics
Gargi College
Siri Fort Road,
New Delhi-110049, India

³Department of Elementary Education
Gargi College
Siri Fort Road,
New Delhi-110049, India

⁴Inter University Accelerator Centre
ArunaAsaf Ali Road,
New Delhi -110067, India

Corresponding Author

(Submitted 07-06-16)

Abstract

The evaluation of Boltzmann constant using V-I characteristics of diodes has been used to understand various aspects of fundamental physics. The use of diodes for analog and digital applications is based on the basic diode characteristics. The use of low-cost devices and tools for interfaced experiments in contrast to traditional methods provide new levels of understanding of the physical concepts. In the present report, the evaluation of Boltzmann's constant has been carried out with the help of an interfacing device, EXPeyes junior (Experiments for Young Engineers and Scientists junior) (IUAC). This device in conjunction with a laptop is well suited to measure, record and analyzedata. The Python has been used for coding. The data has been analyzed with the Xmgrace. The V-I data of the silicon diode IN4001 has been obtained. The value of Boltzmann constant is in agreement with the standard value. This unique way of performing the experiment supplements as well as complements the traditional way of performing experiment. This also emphasizes the use of inexpensive devices, power of computing and analysis using easily accessible open software for better performing and understanding of physics experiments.

1. Introduction

The use of ICT and interfacing of experiments is paving way for better visualization and understanding of physics as well as mathematical equations. These provide better description of various phenomena, states and processes. It is also coupled with better accuracy and precision as compared to conventional instruments. The errors in data collection are minimized in comparison to manual collection of data. The inherent features of low- cost and flexibility widen the prospects of inclusion for marginalized societies.

With the accessibility of computers and mobiles, low cost interfacing devices are improving the teaching-learning processes. The EXPeyes junior (Experiments for Young Engineers and Scientist) [1] also offers advantages such as open ended learning, interfacing of various branches such as Physics, Electronics, Computers and Mathematics for real-life applications.

The conventional way of performing V-I characteristics needs power supply, voltmeters and ammeters. The applied voltage and current are measured in the circuit.

The V-I characteristics of diodes are non-linear in nature. The variation between applied voltage and current in the circuit does not obey ohm's law. The data analysis of V-I measurements also provide useful information. The knee voltage, reverse saturation current and Boltzmann's Constant can be evaluated by performing this experiment.

The forward characteristics of a p-n junction diode traditionally are obtained by connecting the positive of the battery to the p side and negative of the supply to the n side of the p-n diode [2]. Voltage is measured across the diode using a voltmeter (0-1 V) and current is measured in the

circuit using an ammeter (0-100 mA). The manual measurements are limited by the least count of the instruments and it affects calculation of Reverse saturation current (~ Microamperes) due to very low value [2].

In contrast, the interfaced experiment can be performed using EXPeyes junior, required components and a laptop/desktop. This method can

be used for obtaining better data and accuracy. The details are given as below.

Description of Expeyes Junior

EXPeyes Junior has been developed by Inter University Accelerator Center(IUAC) and it is interfaced and powered by the USB port of the computer. It has programmable digital and analog inputs, current source and can perform measurements with Python as an interface between the hardware and user [3]. It is worth to mention that coding in Python is quite simple yet apt in performance [3]. It can be downloaded freely on various platforms. A number of experiments can be performed using various features integrated on the EXPeyes junior board. In the present investigation a detailed study is carried out to measure, record and analyze the data for determining Boltzmann's constant. In contrast to conventional ways of performing experiment, this method offers many advantages and help the students to understand the basics of Physics with the aid of electronics, computer and simulations. The data has been fitted using Xmgrace [4] using the standard Diode Equation and various parameters such as Reverse Saturation Current and Boltzmann Constant have been evaluated.

Circuit Diagram

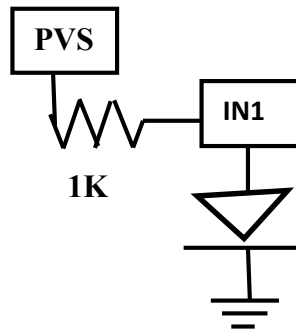


Figure 1. The Circuit Diagram (using EXPeyes junior)

PVS - Programmable Voltage Source
IN1- For reading Voltage

2. Conventional Vs. Automated data

The EXPeyes junior can conveniently set the voltage of PVS (Programmable Voltage Source) in the steps using the python coding (in place of manual variation of voltage). The voltage is read by IN1 as shown in Fig.1 and the python coding, 'iv.py'. The current measurement is done by observing the voltage drop across 1K resistor. The measured current has been calculated by dividing the voltage drop by 1 Kohm resistor value.

#Code in Python (iv.py)

```
from pylab import *
import expeyes.eyesj, time
p=expeyes.eyesj.open()
voltage=[]
current=[]
f=open('diode_iv.dat','w')
v=0.0
while v<= 5.0:
    va=p.set_voltage(v) # set voltage
    time.sleep(.001)
    vd=p.get_voltage(3) # read voltage
    (IN1)
    i=(va-vd)/1.0 # current in
    milliamps
    voltage.append(vd)
    current.append(i)
    ss='%5.3f\t%5.3f'%(vd,i)
    printss
    f.write(ss+'\n')
    v=v+.050 (# 50 mV step size for
    va)
plot(voltage, current)
show()
```

Results

The a forward biased diode, the Voltage-Current Equation [5] is governed by the following expression

$$I = I_0 \left[\exp\left(\frac{qV}{\eta k_B T}\right) - 1 \right] \quad (\text{Eq. 1})$$

For a forward biased region, the Equation reduced to

$$I = I_0 \exp\left(\frac{qV}{\eta k_B T}\right) \quad (\text{Eq. 2})$$

Where

I_0 = Reverse Saturation Current

I = Measured Current; V = Applied Voltage;
 q = electronic charge; η = Ideality Factor = 2 (for Si Diode [6]); k_B = Boltzmann's Constant; $T = 300$ K

After making the circuit (Figure 2), the program was run on the Linux terminal with the following command \$ python iv.py.

The graph started showing the V-I characteristics of the diode instantaneously

on the screen. The data of the experiment was obtained in a file. The V-I characteristics of the diode are shown in Figure 3. The data was exported to Xmgrace (an open access software) and fitting was done using the Equation,

fitting was done using Xmgrace and a_0 and a_1 were evaluated using the fitting.



Figure 2. Automated Set-up. The circuit, Expeyes and Data acquisition on the computer

The representative of the Diode Equation as $y = a_0 \exp(a_1 * x)$ (Eq. 3)

A comparison of Eq.3 with Eq.2 provides the following values

$$a_0 = I_0 \quad (\text{Eq.4})$$

$$a_1 = \frac{q}{\eta k_B T} \quad (\text{Eq.5})$$

The initial guess was inserted for the values of a_0 and a_1 with tolerance of 0.01. The

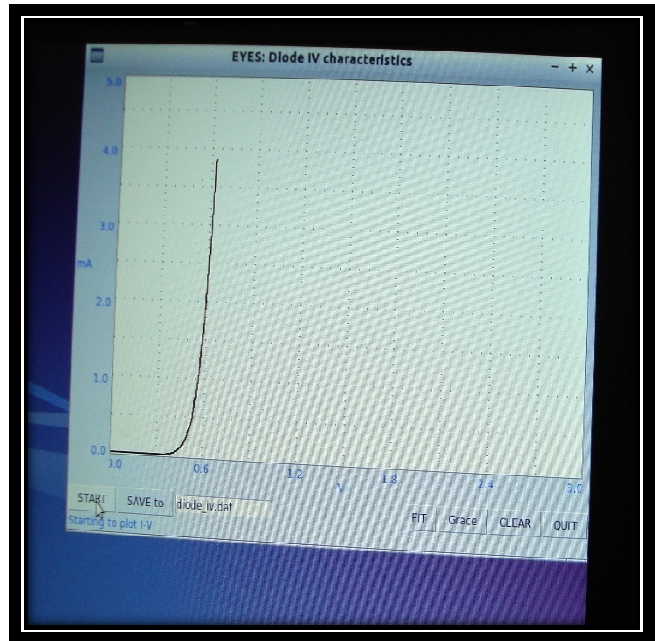


Figure 3. V-I characteristics acquired

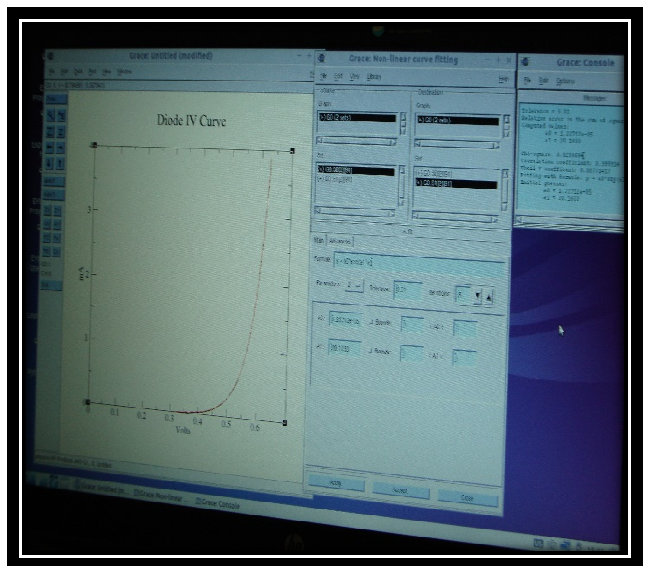


Figure 4 : Fitting using Xmgrace

The following characteristics typical of a diode were observed

1. Upto a certain voltage, there is no increase in current with increase in voltage.
2. After onset voltage, the current increases exponentially.
3. The knee voltage has been calculated by extrapolating the straight line to meet the x-axis. (0.54 volts)

Xmgrace facilitates the fitting of observed data into exponential form $a_0 \cdot \exp(a_1 \cdot x)$. This yields two parameters as follows

$$a_0 = 1.227e-05 \text{ mA}$$

$$a_1 = 20.1033$$

Chi-square: .0238664

Correlation coefficient: 0.999914

$$k_B = \frac{1.6 \times 10^{-19} \text{ C}}{20.1033 \times 2 \times 300 \text{ K}} = 1.326 \times 10^{-23} \frac{\text{J}}{\text{K}}$$

References :

[1] <http://expeyes.in>.

[2] Electronics Principles by Albert Malvino and David Bates, 8th Edition, Mc-Graw Hill, 2015.

[3] <http://www.python.org>

By substituting these values in Eq.2, the value of Boltzmann's constant was calculated, which is in good agreement with the standard value of $1.38 \times 10^{-23} \text{ J/K}$.

Discussion:

The interfacing of experiments reconsolidates the theoretical knowledge. The errors incorporated in acquiring the data are minimized with the automated data. The programming in Python provides a versatility due to simple syntax. The usability of such low-cost devices and other freely available software & tools could be well exploited further for improving physics education mediated through more visualization.

Acknowledgments

The thanks are due to the grant from Innovation Project GC-301 from University of Delhi to Gargi College.

[4] [https://en.wikipedia.org/wiki/Grace_\(plotting_tool\)](https://en.wikipedia.org/wiki/Grace_(plotting_tool))

[5] Solid State Electronics Devices by B. G. Steetman and S.K Banerjee, 6th Edition, PHI

[6] Integrated Electronics : Analog and Digital Circuits and Systems by Jacob Millman and Christos C Halkias, McGraw-Hill Electrical and Electronic Engineering Series

Magnetic Actuators in order to study Faraday Force

Takuo Sakon, Seiji Nitabaru, Takahiro Higasa, Yasushi Hara and Keisuke Nakagawa

Department of Mechanical and System Engineering,
Faculty of Science and Technology,
Ryukoku University, 1-5Yokotani, Seta,
Otsu City, Shiga Pref., 520-2194, Japan

Email: sakon@rins.ryukoku.ac.jp

(Submitted: 13-May-2016)

Abstract

We developed basic magnetic actuators that use the Faraday force by the magnetic field gradient. These actuators can be used in physics experiments for physics or engineering students. A conical coil was made by winding up a copper wire around a polyimide tube; electric current through the coil induces a magnetic field. Using magnetic actuators, students can study the relationship between the magnetic field gradient and Faraday force.

Keywords: Faraday force, magnetic field gradient, ferromagnet.

1. Introduction

Understanding magnetic force is one barrier to dealing with electromagnetism. In the subfield of condensed matter physics that investigates strongly correlated $4f$ and $5f$ electrons systems, electric field gradients are used to explain the interactions in electric quadrupoles and octapoles of atoms and ions. In regard to magnetic forces, the phenomenon of a magnet attaching to an iron plate occurs due to the magnetic field gradient. This article describes experiments conducted using coils and small iron rods that students can perform to understand the relationship between magnetic force and magnetic field gradient. Conducting wire was wound around a thin pipe made of polyimide resin to make a coil. A magnetic field and a magnetic field gradient were produced by passing an AC current through

the coil. A small metal rod placed in the pipe vibrates on the application of current. In this experiment, magnetic force and potential from a magnetic field in the coil, which was generated by AC current and a magnetic field gradient, and the quantitative consideration reached about a phenomenon to vibrate. The magnetic force caused by the magnetic field gradient causes a magnet to attaches to magnetic bodies such as iron. The magnetic force called as Faraday force is written as [1]

$$F_m = \frac{1}{2} \frac{\chi_m}{\mu_0} \frac{\partial B^2}{\partial x} V = \left(\frac{\chi_m}{\mu_0} V \right) \cdot B \frac{\partial B}{\partial x} \quad (1)$$

where χ_m is magnetic susceptibility, V is the volume [m^3], B is the magnetic flux density [T], and μ_0 is the magnetic permeability of vacuum.

Several scientific apparatuses use magnetic field gradients, for example, apparatuses for magnetic measurement, magnetic field generators, and nuclear magnetic resonance (NMR) and magnetic resonance imaging (MRI) apparatuses.

1. Magnetization measuring system using a magnetic field gradient.

Capacitance-type magnetometers can be used to measure magnetization [2]. A large magnetic field gradient occurs in the centre of the main coil where the sample is placed. The sample then experiences a large magnetic force in proportion to magnetization, which causes it to displace. The displacement is measured using by the capacitance method, and the magnetization is inferred based on the displacement.

2. Local large magnetic field generator [3].

A magnetic field generator that can produce a large magnetic field of the sub-tesla degree in the minute domain of the nanometre degree. A magnetic field gradient of up to 1MT/m was produced by diverting an electric current to each conducting wire.

3. NMR and MRI instruments.

NMR and MRI instruments, which are used in research and clinical settings, have a magnetic field gradient (slant magnetic field) coil [4]. For example, for medical usage, the magnetic resonance of internal protons (hydrogen atoms) of the patient is important, but the magnetic field at which a proton resonates is fixed and the position of the proton that resonates is identified by generating a gradient in the magnetic field using a magnetic field gradient coil. Because water is easy to collect, the position of the affected part can be identified by the magnetic resonance phenomenon of the proton.

The abovementioned examples are of instruments that use magnetic field gradients and applied magnetic fields, but from a standpoint of the magnetic engineering, the application of a magnetic field to a trembler and a magnetism actuator is more interesting.

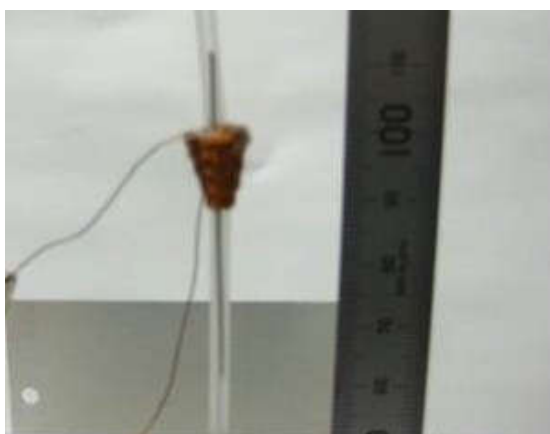
In this study, we developed a magnetic actuator that uses the magnetic force generated by a magnetic field gradient, which can be used in physics experiments for physics or engineering students. Specifically, we fabricated a conical coil by winding a copper wire around a polyimide tube and passed an electric current through the copper wire. Because a magnetic field is generated inside a coil when an electric current was applied to the coil, a rod placed in the coil vibrates. Thus, a magnetic actuator that uses this vibration phenomenon was developed.

2. Experimental, Results and Discussion

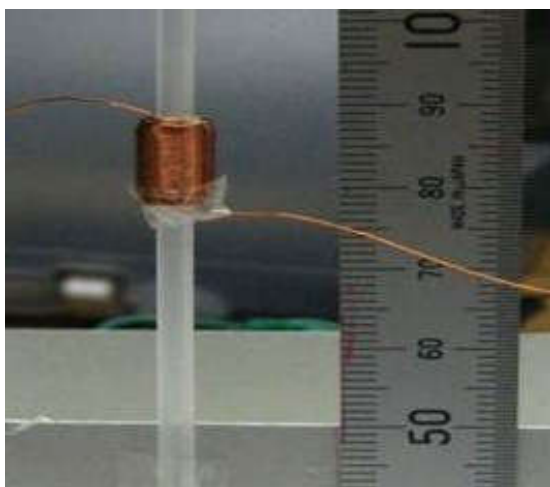
2.1. Vertical magnetic actuators

To observe the Faraday force, two kinds of coils were used. One was a conical coil and the other was a uniform winding coil. Both coils were made by using polyimide-coated copper wire (0.2 mm in diameter) wound around a thin plastic cylinder that has a 2.5mm outside diameter and a 1.6mm inside diameter, as shown in Figure 1. For making the conical coil, copper wire was wound up at the first level 50 volumes, the second level 45 volumes, ..., the 5th level 30 volumes, the 6th level 20 volumes, the 7th level 15 volumes, ..., and the 9th level 5 volumes. The total number of volumes was 250. The uniform winding coil was wound 50 volumes at 5 levels. The electrical resistivity of each coil was 2.5 Ω . Both the

coils have the same number of total volumes (250). When an AC current with a maximum value of 0.28 A and a frequency of 5.0 Hz was applied to the conical coil, an iron rod (Niraco Co., Ltd., Tokyo, Japan) placed in the coil (rod diameter 0.8 mm; rod length 50 mm) vibrated in the air, as shown in Figure 1(a). However, when the same AC current was applied to the uniform coil, as shown in Figure 1(b), the iron rod fell out of the tube. This is due to a pulling force (Faraday force) that acted on the iron rod in the conical coil. The iron-rod vibration amplitude was 4.8×10^{-3} m and the frequency was 10.0 Hz.



(a)



(b)

FIG. 1:(a) Conical coil.(b) Uniform winding coil.

The vibration of the iron rod was recorded on video. Students can use the video to determine the acceleration of the iron rod by noting the position of the top of the rod in several scenes as well as the corresponding times. The angular frequency ω is equal to $2\pi f = 62.8$ Hz. Therefore, the acceleration a is $A\omega^2 = 19.0$ m/s². The Faraday force F_m is written as

$$F_m = ma_m = m(a+g) \quad (2)$$

Where m is mass of the iron rod (46.3 mg = 4.63×10^{-5} kg), a_m is an acceleration due to the Faraday force, and g is the acceleration due to gravity (9.80 m/s²). Therefore, the Faraday force F_m is 1.30×10^{-3} N. The value of a_m is 28.8 m/s², which is three times larger than that of the acceleration due to gravity. Consequently, a conical coil is useful for magnetic levitation and as a vertical magnetic actuator.

2.2 Horizontal magnetic actuators

2.2.1 Experimental results

The vertical magnetic actuator in Section 2.1 is designed to vibrate vertically. Actuators vibrating horizontally or in oblique direction can also be useful. Two horizontal magnetic actuators were produced and tested. If a conical coil that is identical with the one used in vertical magnetic actuator is used, the rod will experience on only a pulling force into the coil, resulting in movement in one direction. To try to cause an iron rod to vibrate horizontally, two conical coils were used, as shown in Figure 2.

The sample was a 99.95% pure iron rod (Niraco Co., Ltd., Tokyo, Japan), which had

a diameter of 0.80 mm in diameter, a length L of 65.0 mm, and a mass m of 0.2597 g. In regard to the conical coil, copper wire was wound on the polyimide tube, the first level 100 volumes, the second level 95 volumes, ..., the 11th level 55 volumes, the 12th level 45 volumes, the 13th level 40 volumes, ..., and the 20th level 5 volumes. The total number of volumes was 1,000. The uniform winding coil was wound 100 volumes and 10 levels, with a total number of 1,000 volumes, as shown in Figure 3, in order to compare with the conical coils. The dimensions of the conical coils were 2.0 mm outer diameter, 1.7 mm inner diameter, and 20 mm width. The electrical resistivity of each coil was 11.0Ω .

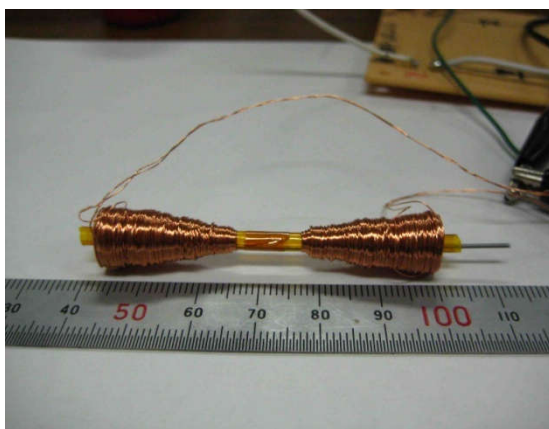
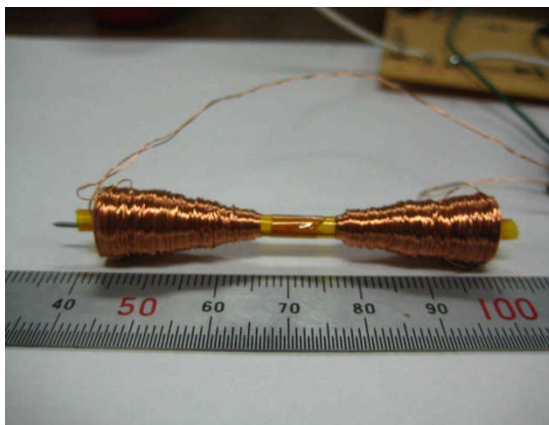


FIG. 2: Actuation of the iron rod by means of two conical coils with a frequency of 5.00 Hz and a function generator voltage output of $1.50 V_{pp}$.

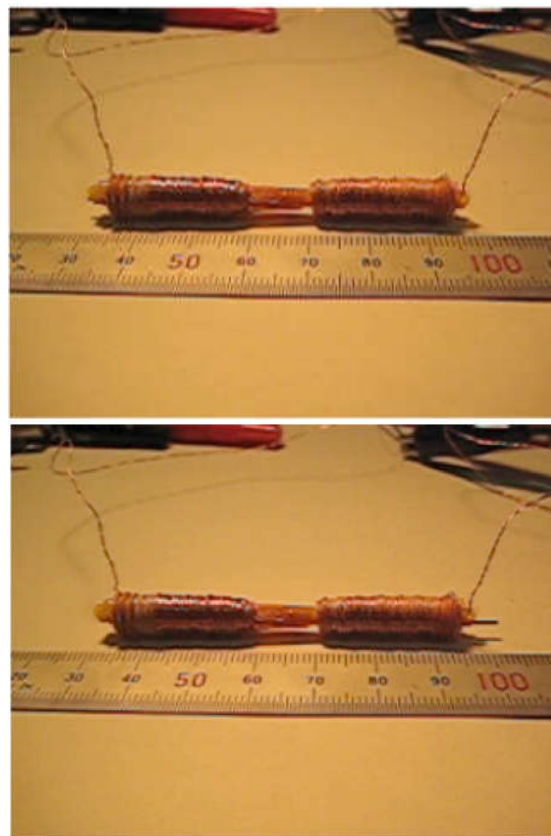


FIG. 3: Actuation of the iron rod by means of two coil of uniform winding with a frequency of 5.00 Hz and a function generator voltage output of $1.50 V_{pp}$.

The circuit for the magnetic actuator is shown in Figure 4. Sine wave voltages were generated using a function generator (NI WF 1943, Yokohama, Japan). An audio amplifier (Marantz PM-17, Chofu, Japan) was also used to stabilize the output voltage. The coils were connected to the audio amplifier via speaker outputs. Diodes were used for half-wave rectification. Therefore, when the L coil was turned on and the magnetic fields applied to the iron rod, the R coil had no current. The results are shown in Table 1. The amplitudes Δx of the conical coil actuator were twice those of the uniform winding coil actuator. This result indicates that the conical coil is effective as a magnetic actuator.

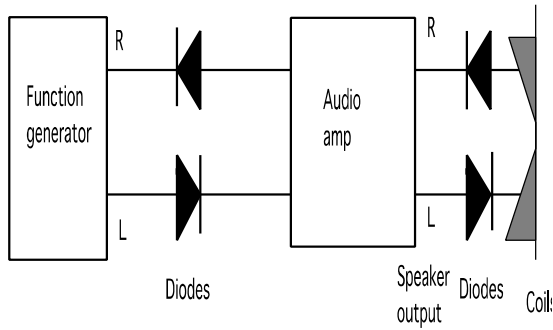


FIG. 4: Circuit for the magnetic actuator.

Table 1. Frequency and voltage dependences of the amplitude of vibration Δx .

Frequency f [Hz]	Function generator output V_{opp} [V]	Coil voltage V_{app} [V]	Uniform winding coil Δx [mm]	Conical coil Δx [mm]
3.00	1.40	2.10	0	6
3.00	1.50	2.50	8	15
4.00	1.40	2.10	5	7
4.00	1.50	2.50	8	18
4.00	1.60	2.90	10	stray out
5.00	1.40	2.10	4	5
5.00	1.50	2.50	8	19
5.00	1.60	2.90	14	stray out

2.2.2 Analysis of the Faraday force

The values of the Faraday force and potential were calculated by using Equation (1). In order to calculate the force, the magnetic susceptibility of their on rod is needed. The magnetic susceptibility was obtained using the magnetization of the rod at various magnetic fields, as shown in Figure 5. From Figure 5, the magnetic susceptibility χ_m was determined to be 5.65. The unit of Wb/m^2 is equal to the unit of T. The density of magnetic flux B [T] is written using the magnetic fields $\mu_0 H$ [T] and the magnetization M [Wb/m^2] as

$$B = \mu_0 H + M \quad (2)$$

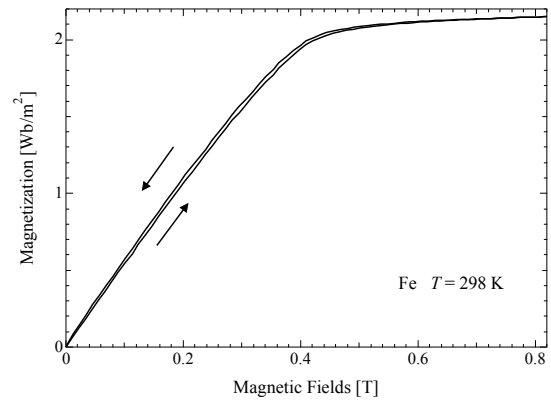
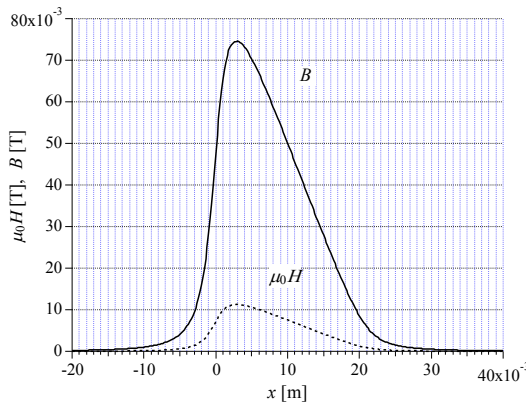


FIG. 5: Magnetization of an iron sample in various magnetic fields.

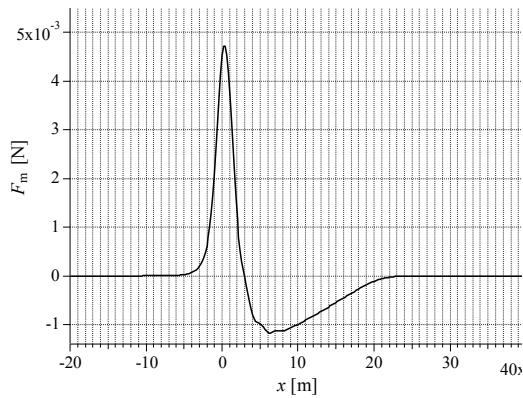
The calculated results of the magnetic field $\mu_0 H$ (by using Biot–Savart law and the density of the magnetic flux B), the Faraday force acting on the iron rod, and the magnetic potential are shown in Figure 6 (conical coil actuator) and Figure 7 (uniform coil actuator). The Faraday force acting on the iron rod in the conical coil is 6.23×10^{-3} N (0.623 gram-force, gf). On the other hand, the Faraday force acting on the iron rod in the uniform winding coil is 2.46×10^{-3} N (0.246 gf). The Faraday force in the conical coil is two and half times larger than that in the uniform winding coil. Moreover, the distance between the lowest points of the potential of the conical coils is longer than that of the uniform coils. Consequently, the range of motion of the iron rod for the conical coils is larger than

that for the uniform coils, as determined by experiments and calculations.

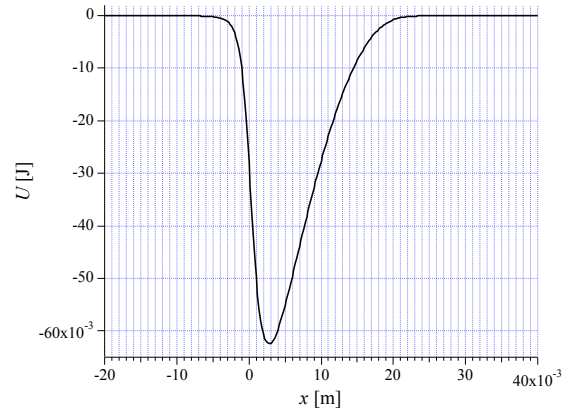
Students become more interested in this experiment when the teachers ask how the strength of magnetic force by which a magnet sticks to an iron plate compares with the strength of magnetic force applied by the magnetic field gradient of this experiment.



(a)

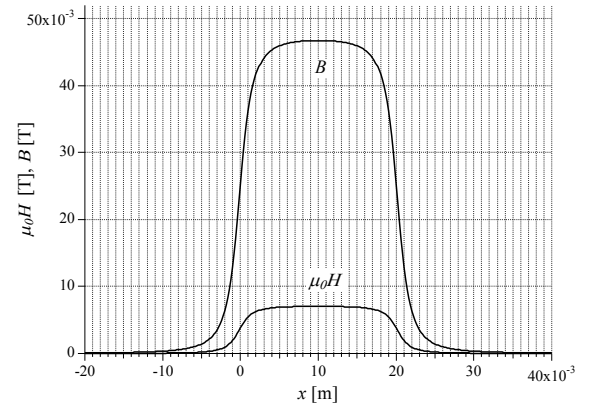


(b)

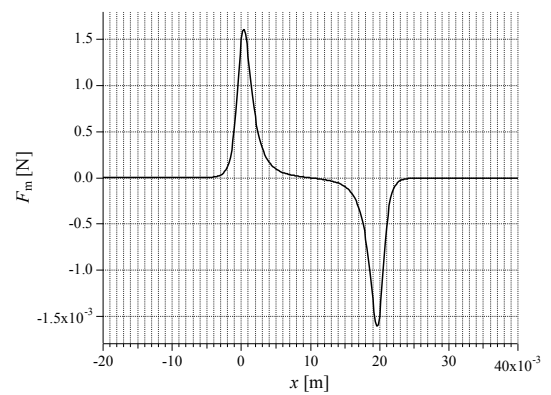


(c)

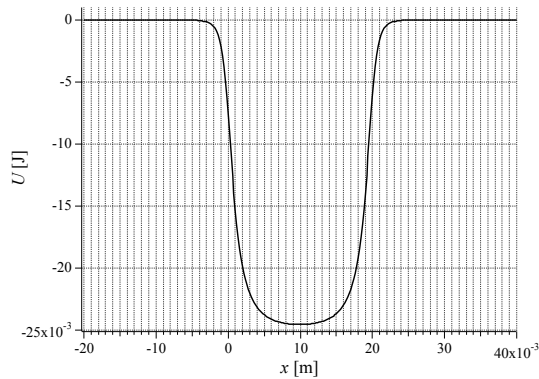
FIG. 6: (a) Magnetic field $\mu_0 H$ and density of the magnetic flux B in the conical coil. (b) Faraday force acting on the iron rod per 1 mm^3 . (c) Magnetic potential of the iron rod per 1 mm^3 .



(a)



(b)



(c)

FIG. 7: (a) Magnetic field $\mu_0 H$ and density of the magnetic flux B in the uniform coil. (b) Faraday force acting on the Iron rod per 1 mm^3 . (c) Magnetic potential of the Iron rod per 1 mm^3 .

3. Applications

We give the two examples of applications of actuators so that students understand the importance of these devices.

3.1 Application of the magnetic actuators

The millimetre-sized micro-miniature trembler is one of the applications of a conical coil. As elucidated in this research, it is small and can make a trembler that generates a large amount of power, especially compared to a uniform coil. A trembler can be used for stirring a solution or a solvent in a micro-laboratory [5].

3.2 Application of the Faraday force under a magnetic field gradient

In mechanical engineering, magneto rheological fluids (MRF) are useful in magnetic dampers and magnetic actuators

[6]. A MRF (e.g., MRF-132LD) is filled in the cylinder of magnetic dampers. A magnetic coil is placed along the flow channel within the piston. Depending on the intensity of the magnetic field in the flow channel, the viscosity of the passing fluid and hence the capacity of the damper changes. An accumulator inside the cylinder accounts for the effective volume change due to the movement of the piston rod. The Faraday force generated by magnetic fields in the magnetic coil induces the flow of the MRF. As described in this paper, when using a conical coil, a large Faraday force is generated. It is inferred that the conical coil can be used for a viscous expensive liquid because the outbreak stress is not small.

4. Concluding Remarks

We developed basic magnetic actuators that use the Faraday force by the magnetic field gradient, which can be used in physics experiments for physics or engineering students. Students can make actuators and perform experiments if copper wire, resin pipes, iron rods, and AC oscillators are available. Cell phone cameras can be used to record videos to determine positions of the iron rods. A conical coil was made by winding up a copper wire around a polyimide tube. Passing an electric current through the coil generates a magnetic field in the coil. When an iron rod is placed horizontally in the axis of the coil, a Faraday force due to the magnetic field gradient acts on the rod when electric current is passed through the coil. This force causes the rod to vibrate. Magnetic actuators were developed based on this vibration phenomenon. The movement of the rod in the vertical direction and vibration were realized with the conical coil. However, a uniform winding coil with the same number of the windings was used, the rod could not stay vertical in the coil and dropped even when AC voltage was applied. The magnitude of the Faraday force by the

conical coil was approximately three times larger than the magnitude of the gravitational force. Furthermore, lateral vibration was realized by placing two conical coils horizontally. The conical coil actuator generated a large Faraday force 6.23×10^{-3} N (0.623 gf), compared to force generated by the uniform coil actuator 2.46×10^{-3} N (0.246 gf). Using the

References

[1]S. Nishijima, J. Magn.Soc.Jpn.**37**(2013) 333-37.

[2]T. Sakakibara, H. Mitamura, T. Tayama, H. Amitsuka, Jpn. J. Appl. Phys.**33**(1994) 5067-5072.

[3]K. Tsubaki, K.Yamaguchi,Physica E, **40**(2008)2220-2221.

[4]M. Abe, Y.Imamura, A. Kurome, M.Terada, Inclined magnetic field coil device and magnetic resonance imaging device, US Patent (US20100321019 A1), application date 29 Jan., 2009.

magnetic actuators, students can study the relationships between magnetic field gradients and Faraday forces. By performing these experiments and analyses, students should learn that the magnetic force is the result of a magnetic field gradient.

Appendix

We have applied a patent in Japan for the devices described in this paper(unexamined patent application No. 2015-126012).

[5]C. D. Burnham,W. M. Dunne Jr., G. Greub, S.M. Novak, R. Patel,Clin.

Chem.**59**(2013) 1696-1702.

[6]S. Soda, N. Iwata, K. Sunakoda, H.

Sodeyama, H. Fujitani,Proc. SPIE's 8th

Annual Int. Symposium on Smart Structures and Materials (2001)4330-24,1-10.

Gibbs paradox: Mixing and non mixing potentials

T. P. Suresh ^{1*}, Lisha Damodaran ¹ and K. M. Udayanandan ²

¹ School of Pure and Applied Physics
Kannur University,
Kerala- 673 635, INDIA
*sureshtp2006@gmail.com

² Nehru Arts and Science College, Kanhangad
Kerala- 671 314, INDIA

(Submitted 12-03-2016, Revised 13-05-2016)

Abstract

Entropy of mixing leading to Gibbs paradox is studied for different physical systems with and without potentials. The effect of potentials on the mixing and non mixing character of physical systems is discussed. We hope this article will encourage students to search for new problems which will help them understand statistical mechanics better.

1 Introduction

Statistical mechanics is the study of macroscopic properties of a system from its microscopic description. In the ensemble formalism introduced by Gibbs[1] there are three ensembles-micro canonical, canonical and grand canonical ensemble. Since we are not interested in discussing quantum statistics we will use the canonical ensemble for introducing our ideas. To study the thermody-

namics of any system (which is the main aim of statistical mechanics) we need to calculate the canonical partition function, and then obtain macro properties like internal energy, entropy, chemical potential, specific heat, etc. of the system from the partition function. In this article we make use of the canonical ensemble formalism to study the extensive character of entropy and then to calculate the entropy of mixing. It is then used to explain the Gibbs paradox. Most text books

[2, 3, 4, 5, 6, 7, 8, 9] discuss Gibbs paradox considering only the case of the classical ideal gas, but here we analyze different physical systems with and without potentials. The study of Gibbs paradox is very fundamental as pointed out by Erwin Schrödinger- “It has always been believed that Gibbs paradox embodied profound thought. That it was intimately linked up with something so important and entirely new could hardly have been foreseen.”

2 Gibbs paradox

When entropy of an ideal gas was calculated using ensemble theory, it was found to be not extensive.

$$S = N k \left[\ln \left(\frac{V}{\lambda^3} \right) + \frac{3}{2} \right].$$

The entropy of mixing for two ideal gases is the difference between the total entropy after mixing and that of individual systems before mixing. For the same particle density, the entropy of mixing is given by

$$\Delta S = k \left[N_1 \ln \frac{N_1 + N_2}{N_1} + N_2 \ln \frac{N_1 + N_2}{N_2} \right].$$

If we find ΔS for two different ideal gases it is found that there is a finite entropy of mixing, but a paradoxical situation is there for similar ones - instead of getting $\Delta S = 0$ there is a finite entropy of mixing. Thus the non extensive character of the entropy equation causes the Gibbs paradox when there is mixing. This paradox is resolved in an ad hoc way by Gibbs. He put a correction factor $N!$

in the denominator of the partition function. The corrected N particle partition function is

$$Q_N = \frac{Q_1^N}{N!},$$

where Q_1 is the single particle partition function.

With this correction the entropy become extensive which resolves the paradox.

$$S = N k \left[\ln \left(\frac{V}{N \lambda^3} \right) + \frac{5}{2} \right].$$

The entropy of mixing then turns out to be

$$\begin{aligned} \Delta S = & k \left[(N_1 + N_2) \ln \frac{V_1 + V_2}{N_1 + N_2} \right] \\ & - k \left[N_1 \ln \frac{V_1}{N_1} + N_2 \ln \frac{V_2}{N_2} \right]. \end{aligned}$$

If the initial particle densities of two similar mixing systems are equal, this equation gives $\Delta S = 0$. The recipe of Gibbs corrects the enumeration of micro states as necessitated by the indistinguishability of identical particles [3].

3 Thermodynamics in the canonical ensemble

In the canonical ensemble the bridging equation to find the thermodynamics is

$$A = -kT \ln Q_N,$$

where A is the Helmholtz free energy, k is Boltzmann's constant and T is the absolute

temperature. To circumvent Gibbs paradox the above equation is modified as

$$A = -kT \ln \frac{Q_N}{N!}.$$

Using Stirling's approximation, $\ln N! = N \ln N - N$,

$$A = -kT (\ln Q_N - N \ln N + N).$$

With the inclusion of Gibbs' correction factor A contains new terms which are T and N dependent. So the entropy (S) given by the equation

$$S = - \left(\frac{\partial A}{\partial T} \right)_{V,N}$$

needs to be modified. In the coming sections we will consider different systems with and without potentials which can be grouped into mixing and non mixing systems as relevant to the Gibbs paradox. The systems are classified as

1. Free classical particles
2. Particles in a potential without Gibbs paradox
3. Particles in a potential with Gibbs paradox

In these sections we will connect the effect of potentials on entropy of mixing by finding the extensive nature of entropy for different physical systems.

4 Free classical particles

Free particles can be

1. Non-relativistic free particles
2. Massive particles with a relativistic formulation
3. Ultra relativistic

4.1 Non-relativistic

For a single non-relativistic particle, the energy is

$$E = \frac{p^2}{2m}$$

and the N particle partition function is

$$Q_N = \left(\frac{V}{\lambda^3} \right)^N,$$

where V is the volume and λ is the de Broglie thermal wavelength given by

$$\lambda = \frac{h}{(2\pi m kT)^{\frac{1}{2}}}.$$

The entropy is

$$S = N k \left[\ln \left(\frac{V}{\lambda^3} \right) + \frac{3}{2} \right]$$

which is not extensive. Introducing the Gibbs correction factor $\frac{1}{N!}$ in the N particle partition function we get

$$Q_N = \frac{1}{N!} \left(\frac{V}{\lambda^3} \right)^N$$

and entropy becomes

$$S = N k \left[\ln \left(\frac{V}{N \lambda^3} \right) + \frac{5}{2} \right] \quad (1)$$

which is extensive.

4.2 Massive particles with a relativistic formulation

For relativistic particles the energy is

$$\epsilon_p = \sqrt{p^2 c^2 + m^2 c^4}$$

For massive particles $mc^2 \gg pc$ and the partition function is

$$Q_N = \left[\frac{V}{\lambda^3} e^{-\beta m c^2} \right]^N,$$

where $\beta = \frac{1}{kT}$, and the entropy is

$$S = Nk \ln \left[\frac{V}{\lambda^3} e^{-\beta m c^2} \right] + \frac{3}{2} Nk + \frac{N}{T} m c^2$$

which is not extensive. With the Gibbs correction factor the entropy becomes

$$S = Nk \left[\ln \left(\frac{V}{N \lambda^3} \right) + \frac{5}{2} \right]$$

which is same as in Eq.(1).

4.3 Ultra relativistic

Here $pc \gg mc^2$ and the partition function is

$$Q_N = \left[\frac{8\pi V}{h^3} \left(\frac{kT}{c} \right)^3 \right]^N.$$

The de Broglie thermal wavelength is

$$\lambda_r = \frac{hc}{2\pi^{\frac{1}{3}} kT}.$$

So

$$Q_N = \left[\frac{V}{\lambda_r^3} \right]^N.$$

Using this partition function if we calculate the entropy we will get it as not extensive but intensive. Introducing the Gibbs correction factor the entropy becomes

$$S = Nk \left[\ln \left(\frac{V}{N \lambda_r^3} \right) + 4 \right].$$

which is clearly extensive.

The above calculations show that all types of free particles exhibit the Gibbs paradox if the Gibbs correction factor is not used.

5 Particles in a potential

In the coming two sections we will check what will be the effect of potentials in the system to the extensive character of entropy and thereby to the Gibbs paradox.

5.1 Particles in a potential without Gibbs paradox

1. Particles in a harmonic potential

Consider an array of equally spaced N harmonic oscillators along a finite length L with one particle per harmonic oscillator site. The Hamiltonian for a single particle is

$$H = \frac{p^2}{2m} + \frac{1}{2} K x^2$$

where K is the spring constant given by $K = m\omega^2$, where m is the mass of the particles and ω its angular frequency.

The single particle partition function is

$$Q_1 = \frac{1}{h} \int_{-\infty}^{\infty} e^{-\beta \frac{p_x^2}{2m}} dp_x \int_{-L/2}^{L/2} e^{-\beta \frac{Kx^2}{2}} dx$$

$$= \frac{kT}{\hbar\omega} \text{Erf} \left(\sqrt{\frac{\beta K L^2}{8}} \right)$$

In the thermodynamic limit $N, L \rightarrow \infty$ and N/L is finite, the $\text{Erf}(\infty) = 1$, so for the infinite length the single particle partition function reduces to

$$Q_1 = \frac{kT}{\hbar\omega}$$

and then

$$Q_N = (Q_1)^N.$$

So the entropy is

$$S = Nk \left[1 + \ln \frac{kT}{\hbar\omega} \right],$$

which is extensive even without Gibbs correction factor. So there is no entropy of mixing, and in this case the entropy is simply additive. The harmonic potential bounds the particles in the system. When two such systems are in contact no particle flow happens from system to the other. Thus the harmonic potential makes the system non mixing.

2. Quartic oscillator

For a quartic oscillator the Hamiltonian is

$$H = \frac{p^2}{2m} + \frac{1}{2} K q^4.$$

The N particle partition function is

$$Q_N = \left[\Gamma \left(\frac{1}{4} \right) \frac{\sqrt{\pi m}}{2 h K^{\frac{1}{4}}} (2kT)^{\frac{3}{4}} \right]^N.$$

The entropy is

$$S = Nk \left[\frac{3}{4} + \ln \Gamma \left(\frac{1}{4} \right) \frac{\sqrt{\pi m}}{2 h K^{\frac{1}{4}}} (2kT)^{\frac{3}{4}} \right]$$

which is extensive.

3. Anharmonic oscillator

For an anharmonic oscillator the Hamiltonian is

$$H = \frac{p^2}{2m} + Cq^2 - gq^3 - fq^4$$

where C, g and f are positive constants but their values are very small. The N particle partition function is

$$Q_N = \left[\left(\frac{2m}{C} \right)^{\frac{1}{2}} \frac{\pi kT}{h} (X) \right]^N,$$

where

$$X = \left[1 + \frac{3kT}{4} \left(\frac{f}{C^2} + \frac{5g^2}{4C^3} \right) + \dots \right].$$

The entropy is

$$S = Nk \left[1 + \ln \left[\left(\frac{2m}{C} \right)^{\frac{1}{2}} \frac{\pi kT}{h} \right] \right] + Y,$$

where

$$Y = Nk \left[\frac{3}{2} kT \left(\frac{f}{C^2} + \frac{5g^2}{4C^3} \right) + \dots \right].$$

The entropy is extensive.

4. **Electron in a magnetic field**

Consider a system of localized particles of spin half with magnetic moment μ_B , in the presence of an external magnetic field of strength B . The N particle partition function is given by

$$Q_N = [2 \cosh(\beta\mu_B B)]^N .$$

The entropy

$$S = Nk \ln [2 \cosh(\beta\mu_B B)] - Nk [\beta\mu_B B \tanh(\beta\mu_B B)]$$

is extensive.

In all the above calculations we have taken particles which are localized by some potentials which makes the system non mixing so that there is no Gibbs paradox. There is another way to differentiate between mixing and non mixing systems or extensive and non extensive systems. The technique is to draw the single particle phase space trajectories. We can see in Figure 1 that the phase space diagrams of the above localized systems have closed trajectories. This then implies that the systems are non mixing (but the converse is not true as, for example, in chaotic systems).

5.2 **Particles in a potential with Gibbs paradox**

1. **Non-relativistic free particles in a gravitational field**

Consider a collection of N particles of mass m enclosed in a vertical cylinder of

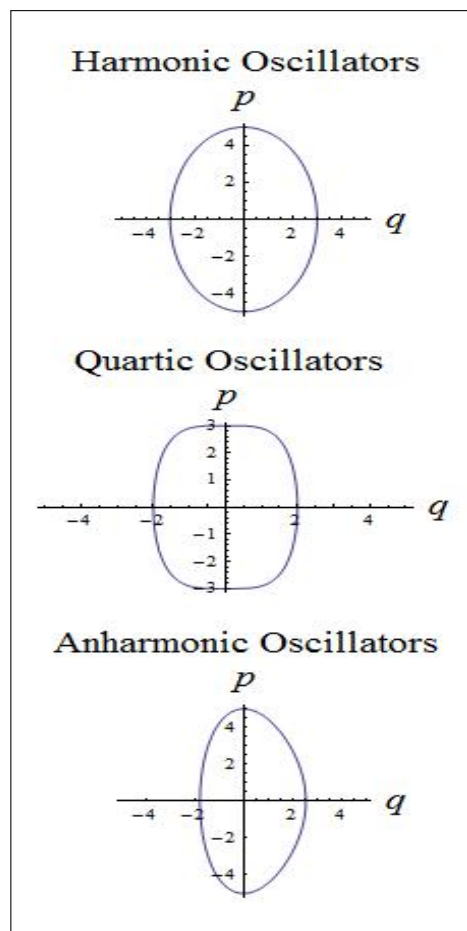


Figure 1: Single particle phase space diagrams

height L in a uniform gravitational field. The total energy of the system is

$$E = \frac{p_x^2 + p_y^2 + p_z^2}{2m} + mgz,$$

where mgz is the gravitational potential energy with z as the height of the particle. The N particle partition function is

$$Q_N = \left[\frac{\mathcal{A}kT}{mg\lambda^3} (1 - e^{-\beta mgL}) \right]^N,$$

where \mathcal{A} is the area of cross section of the cylinder. In the limit when $L \rightarrow \infty$ the partition function becomes

$$Q_N = \left[\frac{\mathcal{A}kT}{mg\lambda^3} \right]^N.$$

The entropy is

$$S = Nk \left[\ln \left(\frac{\mathcal{A}kT}{mg\lambda^3} \right) + \frac{5}{2} \right]$$

which is not extensive. With the Gibbs correction factor the entropy is changed to

$$S = Nk \left[\ln \left(\frac{\mathcal{A}kT}{Nmg\lambda^3} \right) + \frac{7}{2} \right]$$

which is now extensive. If the potential energy is very large the particles will drop to the ground and will become stationary.

2. Diatomic molecule with inter-particle potential

Here we consider a system of diatomic molecules with the 2-particle Hamiltonian given by

$$H = \frac{p_1^2 + p_2^2}{2m} + \varepsilon|r_{12} - r_0|$$

where ε and r_0 are positive constants and $r_{12} = |\vec{r}_1 - \vec{r}_2|$ is the distance between the two particles.

$$Q_1 = \left(\frac{2\pi m}{\beta} \right)^3 V 4\pi X$$

where

$$X = \left[\frac{2r_0^2}{\beta\varepsilon} + \frac{4}{(\beta\varepsilon)^3} - \frac{2e^{-\beta\varepsilon r_0}}{(\beta\varepsilon)^3} \right].$$

$$A = -NkT \ln \left[\left(\frac{2\pi m}{\beta} \right)^3 V 4\pi X \right]$$

and the entropy

$$S = Nk \left[\frac{3}{2} + \frac{Y}{X} \right] + Nk \ln \left[\left(\frac{2\pi m}{\beta} \right)^3 V 4\pi X \right],$$

where

$$Y = \frac{2k(r_0)^2 T}{\varepsilon} + \frac{12kT^3}{\varepsilon} - e^{-\beta\varepsilon r_0} \left(\frac{6kT^3}{\varepsilon} + \frac{2k^2 T^2 r_0}{\varepsilon^2} \right).$$

S is not extensive. With the Gibbs correction factor the entropy is

$$S = Nk \left[\frac{5}{2} + \frac{Y}{X} \right] + Nk \ln \left[\left(\frac{2\pi m}{\beta} \right)^3 \frac{V}{N} 4\pi X \right].$$

We now get an extensive entropy.

3. Diatomic dipoles in external electric field

Consider a system of diatomic molecules with electric dipole moment μ and moment of inertia I placed in external electric field of strength E . The energy of a molecule is given by

$$E = \frac{p^2}{2m} + \frac{p_\theta^2}{2I} + \frac{p_\phi^2}{2I \sin^2 \theta} - \mu E \cos \theta.$$

The N particle partition function is

$$Q_N = \left[\frac{V}{\lambda^3} \left(\frac{I}{\beta \hbar^2} \frac{2 \sinh(\beta \mu E)}{\beta \mu E} \right) \right]^N$$

and the entropy

$$S = Nk \ln \left[\frac{8\pi^2 k^2 T^2 IV}{\mu E \lambda^3} \sinh(\beta \mu E) \right] - \frac{N\mu E}{T} \coth(\beta \mu E) + \frac{7}{2} Nk$$

is not extensive. With the Gibbs correction factor the entropy is

$$S = Nk \ln \left[\frac{8\pi^2 k^2 T^2 IV}{\mu E N \lambda^3} \sinh(\beta \mu E) \right] - \frac{N\mu E}{T} \coth(\beta \mu E) + \frac{9}{2} Nk$$

which is now extensive.

4. Particles with a potential of the form $\frac{1}{2} C |r_2 - r_1|^2$

Consider a system with Hamiltonian

$$H = \frac{p_1^2 + p_2^2}{2m} + \frac{1}{2} C |r_2 - r_1|^2$$

This Hamiltonian approximates a non interacting diatomic molecule. The N particle partition function is

$$Q_N = \left[\left(\frac{2\pi m}{h\beta} \right)^3 V \left(\frac{2\pi}{\beta C} \right)^{\frac{3}{2}} \right]^N.$$

The entropy

$$S = Nk \ln \left[\left(\frac{2\pi mk}{h} \right)^3 V T^{\frac{9}{2}} \left(\frac{2\pi k}{C} \right)^{\frac{3}{2}} \right] + \frac{9}{2} Nk$$

is not extensive. Introducing the Gibbs correction factor the entropy becomes

$$S = Nk \ln \left[\left(\frac{2\pi mk}{h} \right)^3 \frac{V}{N} T^{\frac{9}{2}} \left(\frac{2\pi k}{C} \right)^{\frac{3}{2}} \right] + \frac{11}{2} Nk$$

which is now extensive.

5. Free electrons in a magnetic field

Free electrons in a uniform magnetic field \vec{B} follow a helical path with an axis parallel to the field direction, say, the z axis. The projection on the x, y plane is a circle. The energy associated with the circular motion is quantized in units of $\frac{e\hbar B}{mc}$ and the energy associated with the linear motion along the z axis is taken as continuous. The total energy of such particles is

$$E = \frac{e\hbar B}{2mc} \left(j + \frac{1}{2} \right) + \frac{p_z^2}{2m}$$

where $j = 0, 1, 2, 3, \dots$. The N particle partition function is

$$Q_N = \left[\frac{V}{\lambda^3} \frac{\beta \mu_{eff} B}{\sinh(\beta \mu_{eff} B)} \right]^N$$

where $\mu_{eff} = e\hbar/2mc$ and the entropy is

$$S = Nk \left[\ln \left(\frac{V}{\lambda^3} \right) \frac{\beta \mu_{eff} B}{\sinh(\beta \mu_{eff} B)} \right] + Nk \left[\beta \mu_{eff} B \coth(\beta \mu_{eff} B) + \frac{1}{2} \right].$$

The entropy is not extensive. By introducing the Gibbs correction factor for

the N particle partition function the entropy becomes

$$S = Nk \left[\ln \left(\frac{V}{N\lambda^3} \right) \frac{\beta\mu_{eff}B}{\sinh(\beta\mu_{eff}B)} \right] + Nk \left[\beta\mu_{eff}B \coth(\beta\mu_{eff}B) + \frac{3}{2} \right]$$

which is extensive. The above system is the Landau diamagnetic system in which electrons circulate in a helical path and collide with the walls, and bounce to and fro and behave as free particles.

From the above examples we find that even though these systems are under certain potentials they are non localized and such systems shows the Gibbs paradox.

Conclusions

We have attempted to find the dependence of potentials and their effect on the Gibbs paradox by studying the extensive nature of entropy. It is found that there are potentials which do not allow mixing and for such systems there is no need of the Gibbs correction factor in the N particle partition function. There are some potentials which allow mixing and hence there is a necessity of the Gibbs correction term for the entropy to be extensive. We found that if the equation for the partition function is volume and temperature dependent it can be written as

$$Q_N \propto V\phi(T)$$

for systems which shows the Gibbs paradox, and for systems which do not show the Gibbs paradox

$$Q_N \propto V^0\phi(T)$$

indicating the volume independence and only temperature dependence. In our analysis we found that in the case of free particles, the Gibbs correction is essential to overcome the Gibbs paradox. In the cases of particles confined in a potential like harmonic, quartic, anharmonic potentials, and static electrons in a magnetic field we found that confinement makes the system localized and does not allow particles to flow and so there is no Gibbs paradox. For the systems like free electrons in a magnetic field, non-relativistic free particles in gravitational field and diatomic dipoles in an external electric potential, even if there is a potential there is no confinement, and the system is non localized which allows flow of particles.

Acknowledgement

The authors wish to acknowledge the valuable suggestions provided by the unknown referee, which helped us a lot to modify this article to the present form. T. P. Suresh and Lisha Damodaran wish to acknowledge the University Grants Commission for the assistance given under the Faculty Development Programme.

References

- [1] J. W. Gibbs, *Elementary Principles in Statistical Mechanics*, Yale University Press (1902), reprinted by Dover, New York, 1960.
- [2] Stephen J Blundell and Katherine M Blundell, *Concepts in Thermal Physics*, Second Edition (2010).
- [3] R. K. Pathria and Paul D. Beale, *Statistical Mechanics*, Third Edition, Butterworth (2011).
- [4] Kerson Huang, *Statistical Mechanics*, Second edition, John Wiley and Sons (1987).
- [5] Silvio R. A. Salinas, *Introduction to Statistical Physics*, Springer (2001).
- [6] Roger Bowley and Mariana Sanchez, *Introductory Statistical Mechanics*, Oxford University Press, Second Edition (1999).
- [7] R. P. Feynman, *Statistical mechanics; A set of Lectures*, The Benjamin/Cummings Publishing company, Inc. (1982).
- [8] Herbert B. Callen, *Thermodynamics and an Introduction to Thermo statistics*, Wiley, 2nd Edition (2005).
- [9] Daniel C. Mattis, *Statistical Mechanics made simple*, World Scientific (2003).

Using an iPad to Learn Motion Concepts in Introductory Physics

Tarlok S. Aurora

Department of Mathematics, Physics and Statistics,
University of the Sciences,
600 South 43rd Street,
Philadelphia, PA 19104 USA

(Submitted 05-01-2016)

Abstract

Mobile computing devices such as tablet computers provide an opportunity to record motion of objects with built-in digital video recorders, and to analyze a movie on the device itself. Smartphones can upload a movie to a desktop computer for analysis. This article describes the use of an iPad, Video Analysis and Graphical Analysis apps with examples so that students can learn to explore motion concepts in real life situations; and later share their findings with peers. Examples described here may be used by an instructor in a classroom for purpose of illustration, and to engage students to use their own mobile devices. In the first example described, motion of two balls falling simultaneously was analyzed to show the same rates of fall; and to study kinematics and determine acceleration due to gravity. In the second example, it is shown that circular motion of a ball rolling on a surface, with friction, is equivalent to two damped harmonic motions in two perpendicular directions. In the last example, motion of a foot of person pushing a cart is described. It is suggested that by using mobile digital recorders with traditional experiments, students may gain deeper insight into kinematics and acquire discipline based knowledge.

1. Introduction

Mobile computing devices such as an iPad, tablet computers and smartphones offer a new opportunity to collect and analyze information to facilitate teaching and learning physics concepts in an introductory physics course, both inside and outside a classroom [1, 2]. Motion of an object can be recorded and analyzed on these devices by using Vernier applications such as Video Analysis and Graphical Analysis [3]. If needed, this information may be uploaded to

a desktop computer for a deeper analysis using Vernier's Logger Pro software. A similar analysis application, SparkVue, is available from Pasco [4].

This article describes the use of an iPad to study motion concepts with Video Analysis and Graphical Analysis applications. Three examples and suggestions are presented for use in a classroom to enable students to use their own mobile devices to study motion concepts in a classroom and continue in real life situations. In the first example, motion of

two steel balls dropped simultaneously from the same height - one falling vertically down, and the other one as a projectile – is analyzed to show that the two balls fall at the same rates, and acceleration due to gravity is determined. In the second example, it is shown that a (uniform) circular motion can be decomposed into two (simple) harmonic motions, in two perpendicular directions. In the last example, motion of a foot of person pushing a cart is described. It is shown that by using an iPad along with traditional demonstration equipment one can gain more insight into the underlying physics concepts.

The work described here may be done with the use of a traditional video camera and a desktop PC, but that would not adequately prepare student to use their own mobile

2. Free-fall and projectile motion

The demonstration apparatus, shown in figure 1, is used in a physics classroom to demonstrate that two objects released simultaneously from a given height – one falling vertically down and the other one moving like a projectile – would reach the floor at the same time. When the two balls hit the floor, students hear two simultaneous impacting sounds, thereby proving that times of flight for the two balls are equal. No additional information is obtained from this demonstration when performed in this traditional way [5].

The free fall apparatus consists of a simple arrangement of a horizontal rod with an elastic spring pushing on it. When the rod is pushed against the spring, it is locked in that position with a lever. Two steel balls are placed at the two ends of the rod. When the locking lever is released, the spring forces the rod to move to its original central position. As a result, one ball is released to fall vertically

devices to study motion in real life situations. The work described here was performed by the author on an iPad, and is shared hereto stimulate further exploration of use of mobile technology in a physics classroom. The author has not had an opportunity to use it in a classroom yet, so no student data is included. It is suggested that when an instructor performs these activities in a classroom, students be asked to participate in it by using their own mobile digital recorders, and analyze it using the appropriate free (or affordable) software like Video Analysis and Graphical Analysis. Students may work in small groups to study the motion under teacher's supervision, and later use mobile devices in real life situations for further exploration, and bring back their findings to share with the class.

downward while the other one is launched as a horizontal projectile.



Figure 1. Free-fall and projectile motion demonstration apparatus, shown locked in a “loaded” position.

To study motion of two falling balls with an iPad, the motion was captured with its built-in digital video recorder, against a dark background to enhance visibility. Only one ball can be selected at a time with the help of

the circular cross-hair. In figure 2, both balls are seen to be at the same vertical level during their downward fall, implying that their time of fall toward the floor were equal. In addition, two sounds are heard when the balls hit the floor.

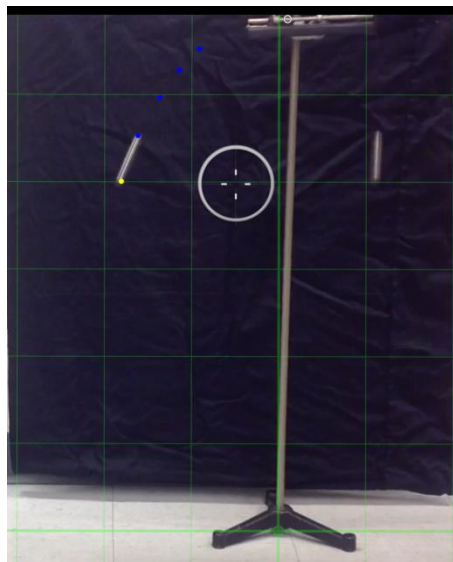


Figure 2. Digital video recording of two balls falling downward. Dots on the left side are the marked positions of the projected ball in several frames of the recording.

For further analysis of the motion recording, the movie was opened in an application named Video Analysis. For the projected ball, positions were marked by tapping on the ball by manually advancing the movie frames. As the ball speeds up, its image becomes a blurred circle with a trail. For consistency, the ball positions were marked at the leading edge of the ball images in all frames. Initial height (position) of the ball is entered in video analysis. Positive y-axis was selected vertically down and x-axis horizontal. Origin was selected at the top - the initial position of the balls. Initial height entered in frame 1 serves as a distance scale in subsequent frames. After the initial height of the ball, with respect to the floor is entered

in Video Analysis, subsequent y-coordinates are calculated by the software. So, parallax was not a concern. The results obtained from data analysis by this application are shown in graphs below. These graphs were saved in a camera roll. In camera roll, the pictures were enhanced by using built-in editing, and were uploaded to a desktop computer for writing purposes.

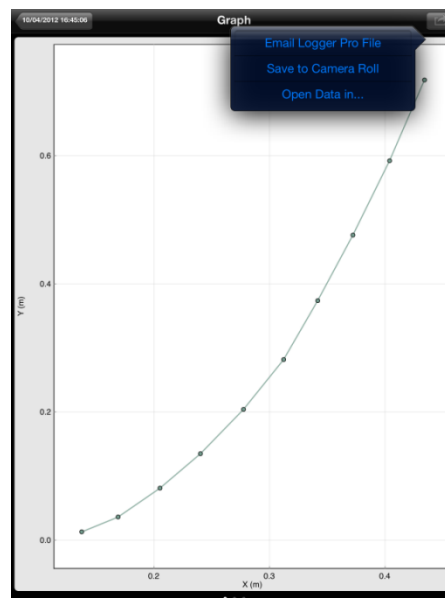


Figure 3. Graph of variation of y-coordinate with x-coordinate.

In Figure 3 shows variation of y with x coordinate. The data points are shown with a connecting line only since regression analysis requires opening data in graphical analysis, by using the “Open Data in” button in figure 3, and which yields figure 4. In figure 4, for the projectile ball, (x, y) graph appears to be a parabola and a quadratic regression line was fitted through it. The x -coordinate varies linearly with time while the y -coordinate is quadratic. Similarly, x -component of velocity appears to be constant while its y -component increases linearly. In figure 4, regression analysis was performed using graphical analysis on the iPad itself and results are shown below.

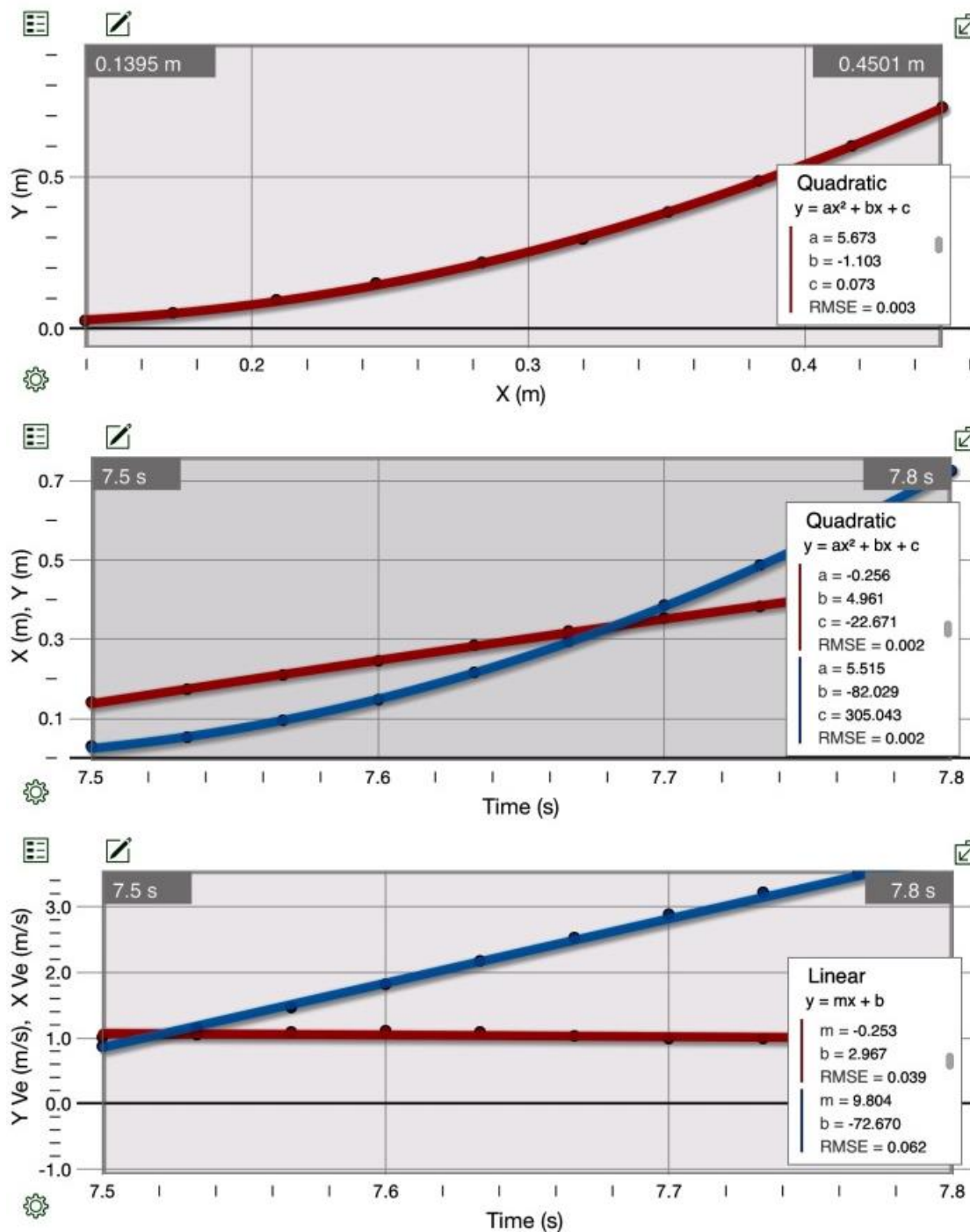


Figure 4. Graphs of x and y components of position and velocity, obtained by opening data in graphical analysis. The top graph is variation of y with x with a quadratic regression line. The middle graph shows variations of x and y coordinates with time, and shown with a quadratic fits. The lower graph shows variation of x and y components of velocity with time, and linear regression lines.

The regression information in figure 4 can be used to understand kinematic equations of motion with zero friction. For this purpose, x-axis is defined in the horizontal plane with y-axis in the vertical direction. (x,y) are position coordinates, and (v_x, v_y) are components of velocity. (a_x, a_y) are components of acceleration, which for a freely falling object are a_x = 0 and a_y = g = 9.8 m/s². Kinematic equations are given below and the subscript o refers to an initial value:

$$x = x_o + v_{ox} t + \frac{1}{2} a_x t^2$$

$$y = y_o + v_{oy} t + \frac{1}{2} a_y t^2$$

$$v_x = v_{ox} + a_x t$$

$$v_y = v_{oy} + a_y t$$

A theoretical plot of these equations with g = 9.8 m/s² and initial values zeros is shown in figure 5, and the graphs resemble the corresponding lines in figures 4.

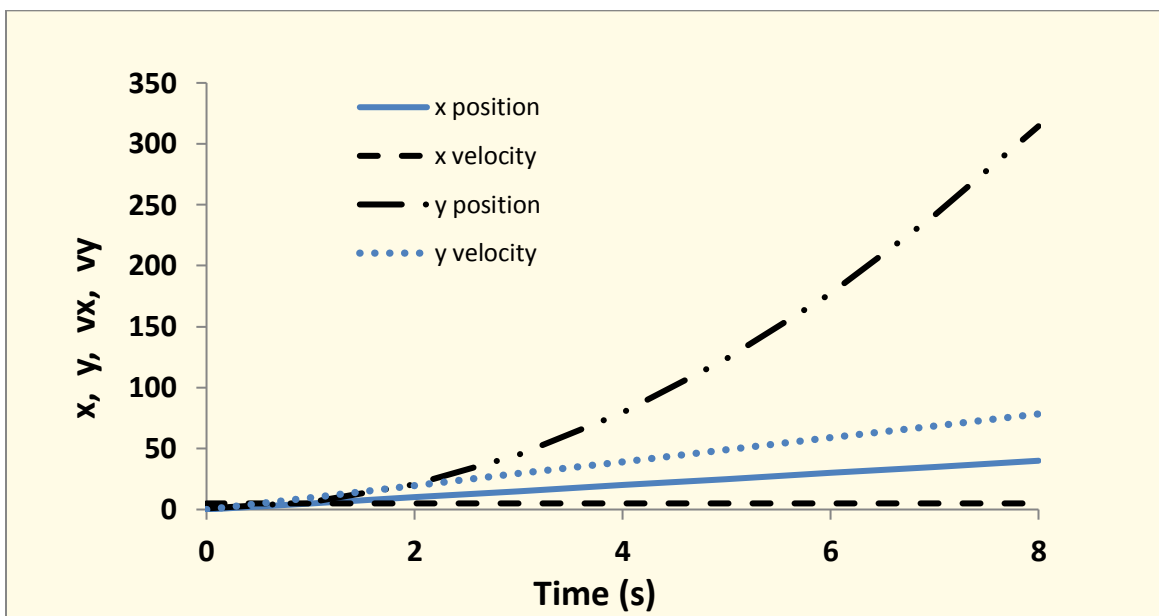


Figure 5: Theoretical graphs for an object moving with a constant acceleration of 9.8 m/s².

From Figure 4, equations and root mean square errors (RMSE) for the regression lines are found to be

$$x = -22.7 + 4.96t - 0.256t^2, \quad RMSE = 0.002$$

$$y = 305 - 82.0t + 5.52t^2, \quad RMSE = 0.002$$

$$v_x = 2.97 - 0.253t, \quad RMSE = 0.04$$

$$v_y = -72.7 + 9.80t, \quad RMSE = 0.06$$

Slope of the v_y graph is 9.8 m/s², which is close to the accepted value of acceleration due to gravity. A small value of acceleration (0.25 m/s²) in the x-direction may be due the fact that the setup was visually aligned horizontal – not with a precision liquid level. The large values of the intercepts are due to the fact that the video recording was started at time zero while the ball was released around 7 seconds, after the author walked over to the free-fall setup. The values from x(t) position graph are not used since it was fitted to a quadratic line (though it is linear)

due to an inability to fit a curve to individual data sets in the graphical analysis app.

Motion of the second ball, falling vertically downward, was similarly analyzed, and figure 6 shows the regression coefficients for it. Value of g is found to be 9.54 m/s^2 from the slope of v_y graph. In figure 6, it is seen that x -coordinate and x -velocity do not change significantly, and have only a slight acceleration in the x -direction for the ball falling vertically down. This small acceleration a_x is perhaps due to an

equipment misalignment with the x - y grid in figure 2 which may have prevented it from falling exactly vertically down; or may be due to vertical axis being not perfectly aligned. The data has not been analyzed for error propagation as the main focus of the article is to prepare students to use their mobile devices to engage in further exploration in real life situations. However, the main source of error lies in marking the positions of the moving ball in a movie, due to blurriness of image, which can be reduced with practice.

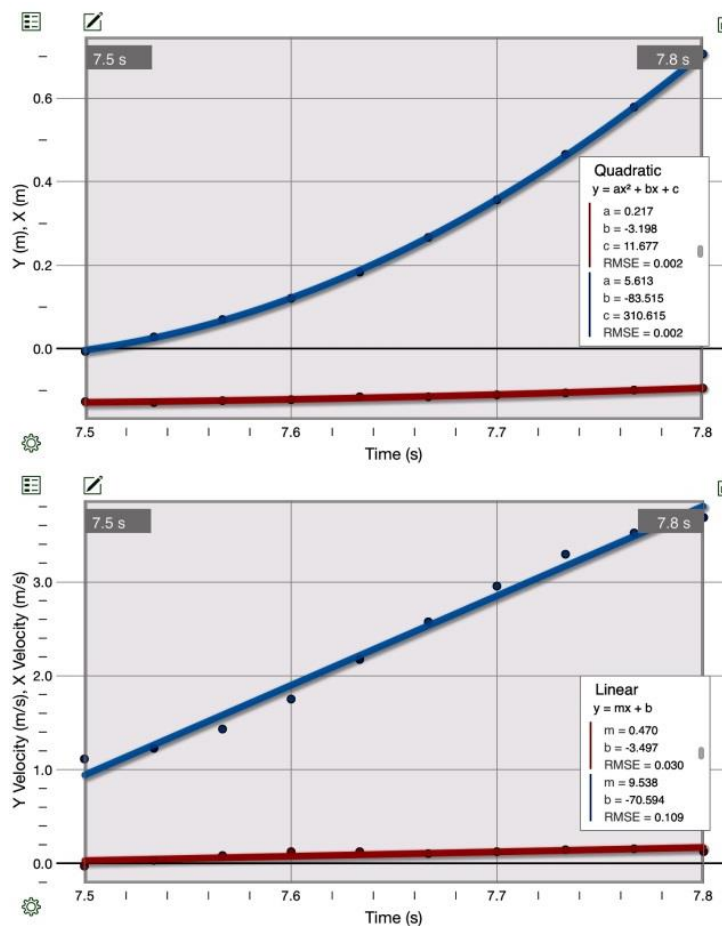


Figure 6. Graphs of motion of a ball falling vertically down. The upper line in both graphs is the y component of position or velocity, and the lower line is the corresponding x -component. Velocity data was fitted to a linear regression line, while a quadratic fit was used for position.

This simple activity shows that by using a digital motion recorder along with a traditional equipment one can demonstrate that both objects fall toward the ground at the same rate (assuming zero or negligible air resistance), learn kinematics and determine acceleration due to gravity.

3. Circular motion

In an introductory physics course, a simple rotational motion is taught by using an object, moving counter-clockwise, in a circular path with a linear (tangential) velocity (v), and a rotational velocity (ω). In figure 7, an object traverses an angular displacement $\theta = \omega t$ in time t . In a classroom, it is shown using trigonometry, that values of x and y component of object's position vector \mathbf{r} and velocity vector \mathbf{v} are given by

$$x = r \cos \theta, \quad y = r \sin \theta$$

$$v_x = -v \sin \theta, \quad v_y = v \cos \theta$$

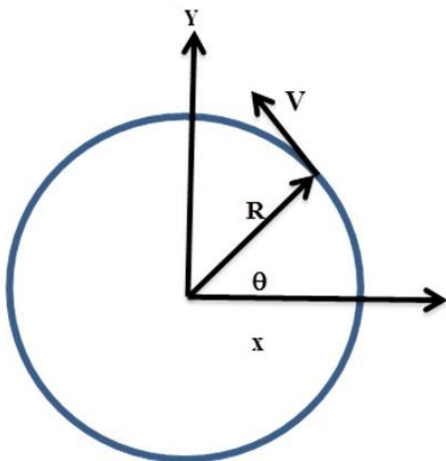


Figure 7. A particle moving in a circular path. R is the radius of the circle, v is tangential velocity, and θ is the angular displacement at time t .

Using properties of trigonometric functions, students learn that position and velocity components are simple harmonic functions, and that sine and cosine functions are 90° ($\pi/2$ radians) out of phase with each other since

$$\sin \theta = \cos(\pi/2 - \theta) \text{ and}$$

$$\cos \theta = \sin(\pi/2 - \theta).$$

To illustrate connection between circular and harmonic motion, often a demonstration apparatus, shown in figure 8, is used.



Figure 8. A demonstration equipment illustrating relation between a circular and harmonic motions.

In this equipment, when a handle is manually turned, one piece moves in a circle along the rim while another connected part is constrained to move along a straight line passing through the center of disc [6] thereby establishing a connection between circular and simple harmonic motions. However, an iPad may be used to gain more insight into the two afore-mentioned motions as follows.

In the iPad example described here, circular motion was recorded and analyzed to illustrate its connection with a harmonic motion, and to show the effect of damping. It is suggested that when an instructor performs this activity in a classroom, students be asked to record the motion on their own mobile devices and analyzed it. In this example, motion of a steel ball rolling around the inner rim of a food bowl lid (a common household item) was recorded. The plastic lid was placed on a horizontal surface and a steel ball was manually set in motion to roll along the rim of the lid. In Video Analysis, origin was selected at the center of the bowl lid, and x and y axes were selected to lie in a horizontal plane. Bowl diameter was about 8.4 cm and lid was 10.5 cm, should one be interested in studying centripetal acceleration. In figure 9, a few marked ball positions are shown, and figure 10 displays the variation of x and y components of position and velocity, obtained from graphical analysis.



Figure9. Positions of ball rolling in a circle in a food lid with Video Analysis.

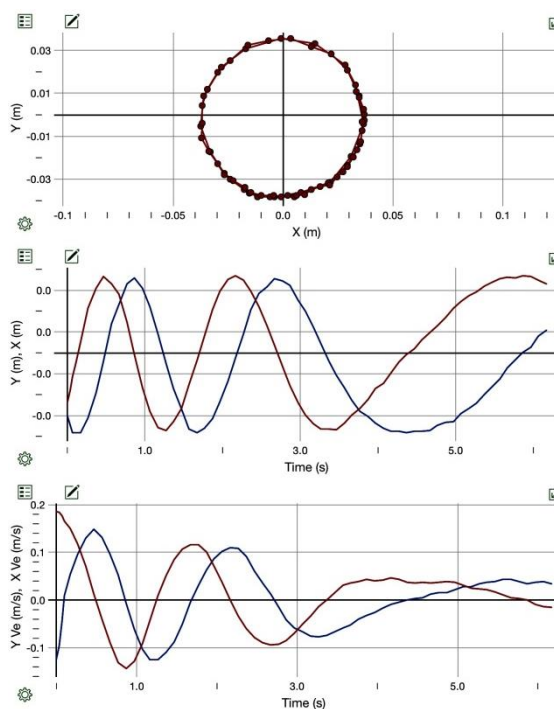


Figure10. The first graph shows a circle which is formed by variation of (x, y) coordinates of a rolling ball. The second graph is variation of x and y coordinates with time and the third graph is variation of velocity components with time. The first graph shows the actual data points while the other two graphs show only the connecting, not the regression lines.

It is seen in figure10that a (uniform) circular motion can be decomposed into two (simple) harmonic motions in two perpendicular directions. In the example shown here, the motion is damped due to the presence of friction. Further, it is seen that position and velocity graphs are 90° degrees out-of-phase. When position coordinates have maximum values at the extreme (turning) points, the corresponding velocities are zero [7]. Trigonometric regression analysis was not done on the graphs due to a lack of this

choice in the app. It is clear that a simple activity like this one can be used to demonstrate several aspects of circular motion.

To demonstrate the mobility of an iPad, a video recording of a person pushing a cart on a boardwalk was made, and analyzed with Graphical Analysis to study position and velocity of a foot during walking. The position of heel of the right foot was marked in video analysis. Length of person's step was estimated to be about 1.0 m. Figures 11 and 12 on the following page show the motion of the heel. The x and y coordinates and the corresponding velocities of the foot are shown to vary as the cart is being pushed to the right side at a steady speed. (Graphical motion of the cart is not shown for the sake of brevity). From the slopes of velocity graphs, one can see that a leg goes through acceleration and deceleration during a leg swing. Such observations can be particularly useful in studying kinesiology for a physical therapy course [8].

To build upon in-class learning, students may be assigned to explore examples of motion in real life situations, such as motion of a flying airplane, roller coaster, simple pendulum, mass on a rubber band or spring (slinky), pendulum clock, child on a slide or swing, water droplet on the wind shield of a car (as a passenger) and a falling leaf. Students could even use smartphones to gather relevant information and upload it to a desktop computer in a physics laboratory for graphical analysis, and to share it with classmates.

Mobile devices may be used in conjunction with the traditional mechanics experiments in an introductory physics course; no need to jettison the old experiments. Briefly, for example, in a laboratory experiment, one may record the sliding motion of a wooden block or cart rolling down an inclined plane to calculate variation of velocity, acceleration and force of friction on the track. Further, by observing the change in velocity and vertical position of the cart on an inclined plane, one could illustrate concept of conservation of mechanical energy and role of friction. In another traditional experiment with a ballistic pendulum, students launch a metal ball projectile from a spring gun, and calculate its launch velocity by measuring its horizontal and vertical displacements when it lands on the floor. With a digital recording of its motion, students could easily observe that the horizontal component of velocity of a projectile stays nearly constant (due to a small air drag) while the vertical component of its velocity changes linearly; just like the ones discussed in the example I in this article.

Other experiments that could benefit from a digital recording are Atwood's machine (for study of Newton's second law), conservation of linear momentum during collisions between two carts on a friction-less track and centripetal force [9]. In conclusion, mobility and ubiquity of iPads and tablet computers offer an easy way to engage students in learning and acquiring discipline-based knowledge, both in and outside a classroom, and promote lifelong learning.



Figure 11. Positions of the right heel of a person pushing a cart.

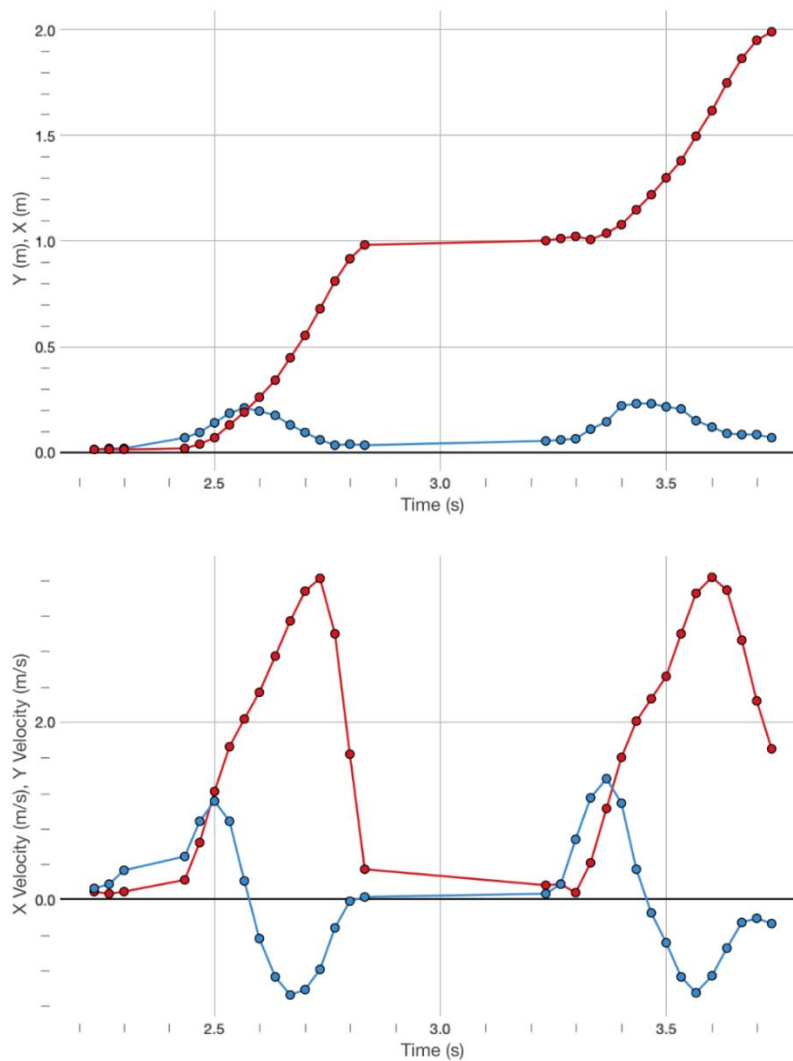


Figure 12. x and y positions and velocities of a heel as the foot moves up, down and forward. Red curve is x component and blue curve is the y component.

Acknowledgments

The author would like to thank University of the Sciences (USciences) for a grant of an iPad; and Rich Cosgriff, Rod Murray and Andrew Esposito, Phyllis Blumberg and Elia Eschenazi for useful discussions.

References:

[1] Klein P, Grober S, Kuhn J and Miller A 2014 Video analysis of projectile motion using tablet computer as experimental tools. *Phys. Ed.* **49** (1) 37

[2] Streepey J January 2013 Using iPads to illustrate the impulse-momentum relationship, *Phys. Teach.* **51**, 54-55

[3] Vernier Software & Technology, 13979 SW Millikan Way, Beaverton, OR 97005.

[4] Pasco scientific, 10101 Foothills Blvd, Roseville, California USA 95747.

[5] Sargent Welch, P.O. Box 92912, Rochester, NY USA 14692.

[6] Griffin and George Ltd. Great Britain.

[7] Aurora T and Brunner B 1991 Phase Relations in a Simple Harmonic Motion, *Phys. Ed.* **26** 382

[8] Winter D, Greenlaw R and Hobson D 1972 Television-Computer Analysis of Kinematics of Human Gait, *Computers and Biomedical Research* **5**, 498-504.

[9] Wilson J and Hernandez C, 2005 *Physics Laboratory Experiments*, Sixth Edition, ISBN: 0-618-38259-3. Houghton - Mifflin Company, New York

Teaching Special Relativity with Real Rotation Matrix

E. Benedetto^{1,2}

¹ Department of Engineering,
University of Sannio,
Piazza Roma 21,
I-82100 Benevento, Italy

² High School T.Tasso Piazza S. Francesco D'Assisi,
1, 84100 Salerno, Italy

(Submitted: 07-06-2016)

Abstract

This brief note has pedagogical motivation and we want to emphasize that an introduction of Loedel representation of space-time, is very useful for high school students to understand the special relativity geometrically. We summarize a series of lectures given at the high school “Torquato Tasso” of Salerno by the author of this paper and by his tutor teacher Rachele Lanzillotti. The aim of this short note is to stimulate curiosity and it wants to be a starting point to explore this topic.

1. Introduction

It is well known that Minkowski introduced the concept of space-time continuum and a geometrical representation of Lorentz transformations is usually studied using his diagrams. In this way it is graphically possible to understand relativistic phenomena even without using mathematical equations [1]. In this approach two inertial observers are represented by an orthogonal system and by a system with oblique axes. Moreover the Minkowski diagram uses different scales for the orthogonal and the non-orthogonal axes and therefore it is necessary to calculate a scale factor to convert the units of a frame into the units of the other one

moving with a constant velocity. All this is often difficult for students. The main attraction of the Loedel Space time diagram is, instead, that it treats the reference frame and the first moving frame symmetrically and hence they have identical scales in geometric units[2],[3],[4]. Furthermore the students can use standard matrix of rotation without recourse to imaginary axes and angles. This approach became known and were studied in more detail by several authors [5],[6],[7],[8],[9] but it is completely ignored in most textbooks. These underused diagrams are fundamental to understanding the real relativistic physical consequences that should not be confused with the change of units that is only a product of the choice of

the graphical representation. We will use a simple way to show the invariance of units of length and time for the two Loedel observers.

2. Galileian space-time geometry

In classical physics the link between the Cartesian coordinates of an object in two inertial reference frames in uniform rectilinear motion relative to one another with velocity v , is given by the Galileian transformations

$$\begin{cases} x' = x - vt \\ t' = t \end{cases} \quad (1)$$

From a geometric point of view, they convert coordinates from Cartesian system to non-orthogonal axes. Indeed the x' axis coincides with the x axis but the t' axis is inclined, relative to the t axis, of $\alpha = \arctg v$. Indeed the points of this axis are those that have null abscissa and therefore are those that are located on the straight line $x - vt = 0$. Furthermore one can easily observe that the point $A'(1,0)$ has still coordinates $(1,0)$ on the (x,t) plane. Instead $B'(0,1)$ has coordinates $(v,1)$ on the (x,t) plane, that is, in this reference, $OB' = \sqrt{1 + v^2} > 1$. So the unit of measure of t' axis is larger than that of the t axis.

3. Relativistic space-time geometry

In special relativity, instead, the link between coordinates is governed by Lorentz transformations

$$\begin{cases} x' = \frac{x - \beta\tau}{\sqrt{1 - \beta^2}} \\ \tau' = \frac{\tau - \beta x}{\sqrt{1 - \beta^2}} \end{cases} \quad (2)$$

and its inverse formulas

$$\begin{cases} x = \frac{x' + \beta\tau'}{\sqrt{1 - \beta^2}} \\ \tau = \frac{\tau' + \beta x'}{\sqrt{1 - \beta^2}} \end{cases} \quad (3)$$

where $\tau = ct$ e $\beta = v/c$.

In this case the situation is further complicated because, with Lorentz transformations, both axes are inclined by the same angle $\alpha = \arctg\beta$. Indeed the x' axis ($\tau' = 0$) is the straight line $\tau = \beta x$ and the τ' axis ($x' = 0$) is $\tau = x/\beta$. Moreover the points $A'(1,0)$ and $B'(0,1)$ have, on the (x,τ) plane, coordinates respectively $(\frac{1}{\sqrt{1 - \beta^2}}, \frac{\beta}{\sqrt{1 - \beta^2}})$ and $(\frac{\beta}{\sqrt{1 - \beta^2}}, \frac{1}{\sqrt{1 - \beta^2}})$. In both cases the unit vectors of the primed axes become long, in unprimed reference, $\sqrt{\frac{1 + \beta^2}{1 - \beta^2}} > 1$. It is necessary to note that this representation may confuse students because there seems to be a privileged observer, assigning to him a system of orthogonal axes. To eliminate this apparent asymmetry, it is known that it is enough to introduce an imaginary time coordinate $i\tau$ transforming Lorentz relations in orthogonal transformations with a rotation angle $\alpha = \arctg i\beta$. In this abstract case the problem is that it is not possible any graphic representation and, therefore, is not useful from a didactic point of view.

4. Real rotation matrix

From the second relation of (3) we have

$$ct' = ct \sqrt{1 - \frac{v^2}{c^2}} - \frac{v}{c} x'$$

and substituting in the first of (3) we get

$$x = \left(\frac{v}{c}\right) ct + \sqrt{1 - \frac{v^2}{c^2}} x'$$

If we pose

$$\frac{v}{c} = \sin\alpha$$

we can write

$$\begin{cases} \tau' = \tau \cos\alpha - x' \sin\alpha \\ x = \tau \sin\alpha + x' \cos\alpha \end{cases} \quad (4)$$

obtaining the standard clockwise rotation of a real angle. This was observed for the first time by Enrique Loedel Palumbo and it is an excellent tool for teaching special relativity. The peculiarity of this rotation is the mix between the axes of the two systems: indeed it is not a rotation of the (ct, x) frame with respect to the (ct', x') frame, but the rotation of (ct', x) with respect to (ct, x') . The main benefit of this approach is that unlike in Minkowski diagrams, the scales of both axes of both frames are identical and we do not have apparent preference of one of the inertial frames.

5. Invariance of unit vectors for Loedel observers

If we have, in primed frame, $A'(1,0)$, then we obtain

$$\begin{cases} 0 = \tau \cos\alpha - \sin\alpha \\ x = \tau \sin\alpha + \cos\alpha \end{cases}$$

getting

$$\begin{cases} \tau = \operatorname{tg}\alpha \\ x = \frac{\sin^2\alpha}{\cos\alpha} + \cos\alpha = \frac{1}{\cos\alpha} \end{cases}$$

Therefore from Pythagorean Theorem

$$OA' = \sqrt{\frac{1}{\cos^2\alpha} - \operatorname{tg}^2\alpha} = \sqrt{\frac{1 - \sin^2\alpha}{\cos^2\alpha}} = 1$$

With similar reasoning, if we have $B'(0,1)$ we obtain

$$\begin{cases} 1 = \tau \cos\alpha \\ x = \tau \sin\alpha \end{cases}$$

and

$$\begin{cases} \tau = \frac{1}{\cos\alpha} \\ x = \operatorname{tg}\alpha \end{cases}$$

getting, also on the (x, τ) plane, $OB' = 1$.

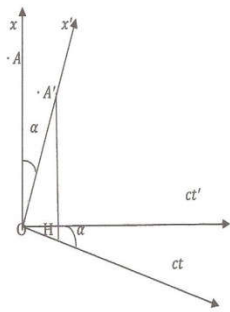


Fig.1: Loedel observers

6. Conclusions

Special relativity theory makes several predictions, some of which seem counter intuitive. The author of this paper has always tried to inspire students so that they could

References :

- [1] T. Takeuchi An Illustrated Guide to Relativity (Cambridge: Cambridge University Press) (2010)
- [2] E. Loedel Aberración y relatividad Ann. Soc. Cient. Argentina 145 3–13 (1948)
- [3] E. Loedel Enseñanza de la Física (Buenos Aires: Editorial Kapelusz) pp 492–8 (1949)
- [4] E. Loedel Física Relativista (Buenos Aires: Editorial Kapelusz) (1955)

themselves infer such phenomena as time dilation and length contraction and requesting the explanation of some “relativistic paradoxes”. For example the Ladder Paradox is a famous thought experiment that shows why you can fit objects into spaces that are too small for them. Students generally have great difficulty and I have verified that they are able to find the right solution, in much more simple manner, through Loedel approach that is often neglected in standard textbooks.

Acknowledgements

The author wishes to thank Prof. Carmela Santarcangelo, Head Teacher of “Torquato Tasso” high school and his Tutor Teacher Prof. Rachele Lanzillotti.

- [5] H. Amar New geometric representation of the Lorentz transformation Am. J. Phys. 23 487-9 (1955)
- [6] H. Amar and E. Loedel Geometric representation of Lorentz transformation Am. J. Phys. 25 326–7 (1957)
- [7] R.W. Brehme A geometric representation of Galilean and Lorentz transformations Am. J. Phys. 30 489 (1962)
- [8] R.W. Brehme Geometric representations of the Lorentz transformation Am. J. Phys. 32 233 (1964)
- [9] A. Shadowitz Special Relativity (Philadelphia, PA: Saunders) (1968)

Book Review:**Quantum Field Theory**

The Why, What and How

ThanuPADMANABHAN

Springer 2016

Graduate TextsinPhysics:ISSN1868-4521(electronic)

ISBN978-3-319-28171-1;ISBN978-3-319-28173-5(e-book)

i-xvii+283pages

Reviewedby

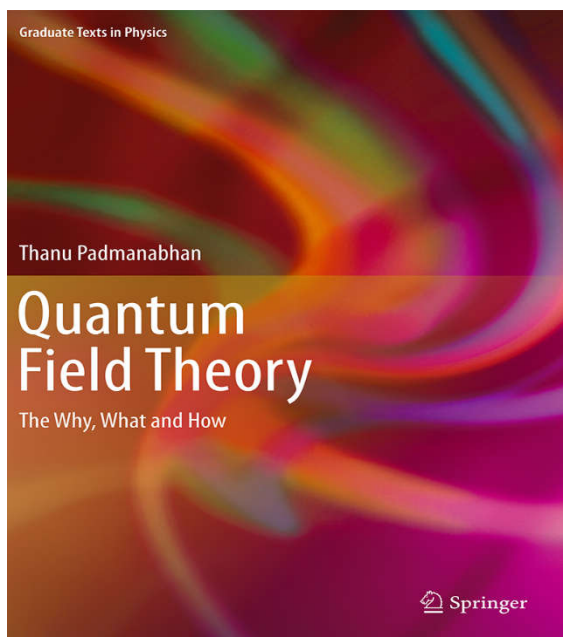
R Ramachandranrr_1940@yahoo.co.in, rr@imsc.res.in)

Formerly

The Institute of Mathematical Sciences, Taramani, Chennai 600113

And

Indian Institute of Technology, Kanpur 208016



What is the need for yet another book on Quantum Field Theory? Is there another way of exposition that clarifies the nuances of the formalism, such that it allows one to appreciate the underlying concepts as well as do practical computations in a more informed way? Padmanabhan, well known as a very effective teacher-communicator, makes a strong case in the

affirmative. Quantum Field Theory is the language in which the basic constituents of all matter gets their dynamics expressed. Hence it is important for all students of Physics to be reasonably well acquainted with it. There are many ways in which this book differs from other introductory text books that every generation of Theoretical Physics Students get exposed to. To get an overview of what is contained in this book, see the “Chapter Highlights” in the very words of the author that follows this review.

Traditionally one begins the subject with the classical Lagrangian Mechanics and picks up the Hamiltonian formalism before one gets to Quantum Mechanics in either Schroedinger picture or Heisenberg picture in the nonrelativistic domain. One uses either position basis or momentum basis and the formalism is similar. However, in the relativistic case the position basis throws up a problem. As particle is localized the uncertainty in its momentum and hence its energy content increases and soon the state necessarily coexists as a state with additional particle – antiparticle pairs that can be created with the available energy. This leads to what one used to refer

as ‘Second Quantization’. From finite dimensional Quantum Mechanics, we end up with Quantum Field theory, with infinitely many variables that constitute a Field. For the simplest Scalar Field, this turns out to be a set of simply infinite dimensional harmonic

oscillators, one for each mode $\omega(\mathbf{p}) = \sqrt{\mathbf{p}^2 + m^2}$. Padmanabhan shows that this emerges naturally when one starts from the relativistic Action for a free particle and ‘quantize’ *ala* path integral mode.

The systematic procedure leads to an appropriate relativistic propagator for the free particle expressed as

$$G(x_2; x_1) = -\frac{1}{16\pi^2} \int_0^\infty \frac{d\mu}{\mu^2} \exp\left(-i(m^2 - i\epsilon)\mu - \frac{i x^2}{4\mu}\right);$$

in contrast the nonrelativistic analogue happens to be $G(x^2; x^1) = \theta(t) \left(\frac{m}{2\pi i t}\right)^{3/2} \exp\left(\frac{i m|x|^2}{2t}\right)$. While the nonrelativistic expression indicates, in view of $\partial(t)$ factor, a causal propagation of a single particle, the relativistic expression admits paths that go both forwards and backwards in time, calling for multi-particle intermediate states. A little analysis shows that they are indeed described by a set of harmonic oscillators (you should wonder where they come from when, we are dealing with a free particle), one for each mode $\omega(\mathbf{p})$. This is a demonstration of the fact that the concept of particle indeed directly leads to Fields. When we later find that Fields, when quantized, reveal particle content in them, particle – wave duality is complete.

One then generally moves on to espousing the real and complex scalar field theory and proceed to study the effect of static electromagnetic field as an example of interaction. Following this one studies perturbative effects of $\lambda\phi^4$ interaction and then graduate to fermionic spin $\frac{1}{2}$ fields and QED.

Padmnabhan prefers to lay the concepts of field theory first and so deals with an approach that uses ‘Effective Lagrangians’ to clarify both the vacuum state to begin with, illustrating Casimir Effect, Schwinger Effect etc. and then the concept of Regularization / Renormalization process, vital to relate the experimental measurements with our theoretical constructs. He makes repeated references

to drive home the notion that the Renormalization is not necessarily to merely deal with the infinities in Field Theories and it is much more than just a procedure to hide infinities in the unobservable parameters of the theory. The way the topic is treated in many contemporary text books may give you an impression that in a perturbative *treatment* of a renormalizable field theory, infinities can be handled order by order and systematically absorbed in a few finitely many parameters of the theory to give sensible predictions of experimentally measurable quantities such as the spectrum, level widths/lifetimes, cross-sections etc. in terms renormalized *physical* parameters. In the Wilsonian formulation, adopted in this book from the very beginning, one trades the bare input parameters such as mass, coupling constants etc. for scale dependent parameters. The dependence of coupling constant $\lambda [\rightarrow \lambda(\mu^2)]$ on the energy scale characterized by the mass² value μ^2 of the physical measurement depends on the β function that characterizes the theory and λ is said to be ‘running’. Usually these topics are postponed to an advanced course and one deals with the basic algorithmic approach to do the computations; but I am very pleased that the author takes them up as elements that can be understood even before one has gets to that stage in Quantum Field Theory.

External electromagnetic field makes its entry as a consequence of generalizing the phase symmetry of a complex scalar field $\phi(x)$. By replacing $\partial_\mu \phi$ by

$D_\mu\phi \equiv (\partial_\mu + iqA_\mu)\phi$, the phase symmetry $\phi \rightarrow e^{-iq\Lambda(x)}\phi$ is recovered if simultaneously $A_\mu \rightarrow A_\mu - i\partial_\mu\Lambda$, together with $F_{\mu\nu} = \partial_\mu A_\nu - \partial_\nu A_\mu$ as the gauge invariant electromagnetic field. The free field Lagrangian that describes the dynamics is then derived as $\mathcal{L}_{em} = -\frac{1}{4}F^{\mu\nu}F_{\mu\nu} = \frac{1}{2}(\mathbf{E}^2 - \mathbf{B}^2)$. While the covariant derivative of the complex scalar field yields interaction with an external electromagnetic field, the quantization of \mathcal{L}_{em} yields photons. The technique calls for the quantization to proceed in a chosen gauge, for example, the radiation gauge defined as $A^0 = 0, \nabla \cdot \mathbf{A} = 0$. The number of propagating fields reduces to 2, in view of the presence of constraints and indeed the gauge invariance. The free field quantization has a spectrum with set of states $\{|n_{k\alpha}\rangle$, one each for oscillators labelled by wave vector \mathbf{k} and polarization index $\alpha = 1, 2$. The expectation value of the Hamiltonian:

$$\mathcal{E} = \sum_{\alpha=1,2} \int \frac{d^3k}{(2\pi)^3} \hbar\omega_k (n_{k\alpha} + 1/2)$$

Covariant quantization of the electromagnetic field gives the expected causal expression for the photon propagator for various gauge choices.

As an aside at this stage, Padmanabhan introduces a section on Spontaneous Symmetry Breaking and the notion of degenerate vacuum state in the $\lambda\phi^4$ theory with negative m^2 parameter and employs it to describe spontaneous magnetization of a ferromagnetic state below Curie temperature. Indeed, these play an important role in electroweak gauge theory to be learnt elsewhere. However the generalization of the U(1) into an SU(N) gauge theory is treated in sufficient details in a subsection to get a feel for what is in store.

After three chapters on systematic exposure of real and complex scalar fields and electromagnetic field, one is ready to take on realistic interactions. Padmanabhan follows here a more conventional track, develops covariant perturbative treatment extracting

the celebrated Feynman rules of the theory. The style of the treatment, however, lays more emphasis on the concepts, relegating algebraic derivations to either mathematical supplements or well directed exercises. It challenges the student to work through the text so that (s)he appreciates the concepts as well as gains confidence as a practitioner.

The fifth and final chapter introduces additional theoretical techniques, one needs to deal with fermions. Most textbooks use relevant canonical quantization and drive home that the fermionic fields and operators obey anti-commutation rules, signaling both antisymmetric expressions in the formulae and attendant (Pauli) exclusion principle. For a systematic path integral derivation, one needs to introduce *grassmanians* (sort of anti-commuting numbers). Padmanabhan introduces them to the extent needed to derive all the fermionic analogues of standard expressions for the scalar (and vector) fields we have encountered in the earlier chapters. Electron propagator obtained using fermionic path integrals, deals with both electrons and positrons, since paths include both forward and backward time progression. One is now ready to take up one loop computations in QED and derive loop corrections to photon propagator, electron propagator as well as the electromagnetic interaction vertex ($ie\gamma^\mu$). The celebrated expression for the anomalous magnetic dipole moment as $g - 2 = \frac{\alpha}{\pi}$, as derived by Schwinger follows as a definite prediction of the formalism.

Having completed the exposition of QED with all its formal attributes, including an explicit expression of the β function, that dictates the way of the coupling parameter varies with scale ($\beta(e) = \frac{e^3}{12\pi^2}$), the author feels that students can get adequate mastery in the field going over a *potpourri* of solved problems.

This reviewer **recommends** warmly the new text book to both discerning teachers and serious students in learning the basics of Quantum Field Theory. It is

certainly not an easy read for a first timer in the field, but packs enough serious content for a serious

student of Physics, even if (s)he is one.

Excerpts from the Book

Chapter Highlights:

1. **From Particles to Fields.** The purpose of this chapter is to compute the path integral amplitude for the propagation of a free relativistic particle from the event x_1 to the event x_2 and demonstrate how the concept of a field emerges from this description. After introducing (i) the path integral amplitude and (ii) the standard Hamiltonian evolution in the case of a non-relativistic particle, we proceed to evaluate the propagator for a relativistic particle. An investigation of the structure of this propagator will lead to the concept of a field in a rather natural fashion. You will see how the standard unitary evolution, propagating forward in time, requires an infinite number of degrees of freedom for the proper description of (what you thought is) a single relativistic particle. In the process, you will also learn a host of useful techniques related to propagators, path integrals, analytic extension to imaginary time, etc. I will also clarify how the approach leads to the notion of the antiparticle, and why causality requires us to deal with the particle and antiparticle together.
2. **Disturbing the Vacuum.** The purpose of this — relatively short — chapter is to introduce you to the key aspect of QFT, viz., that particles can be created and destroyed. Using an external, classical scalar source $J(x)$, we obtain the propagator for a relativistic particle from general arguments related to the nature of creation and destruction events. The discussion then introduces functional techniques and shows how the notion of the field again arises, quite naturally, from the notion of particles

which can be created or destroyed by external sources. By the end of the first two chapters, you would have firmly grasped how and why combining the principles of relativity and quantum theory demands a concept like the field (with an infinite number of degrees of freedom), and would have also mastered several mathematical techniques needed in QFT. These include path integrals, functional calculus, evaluation of operator determinants, analytic properties of propagators and the use of complex time methods.

3. **From Fields to Particles.** Having shown in the first two chapters how the quantum theory of a relativistic particle naturally leads to the concept of fields, we next address the complementary issue of how fields lead to particles. After rapidly reviewing the action principle in classical mechanics, we make a seamless transition from mechanics to field theory. This is followed by a description of the (i) real and (ii) complex scalar fields and (iii) the electromagnetic field. Two key concepts in modern physics — spontaneous symmetry breaking and the notion of gauge fields — are introduced early on and in fact, the electromagnetic field will come in as a classical $U(1)$ gauge field. I then describe the quantization of real and complex scalar fields — which is fairly straightforward — and connect up with the ideas introduced in chapters 1 and 2. The discussion will compare the transition from particles to fields vis-a-vis from fields to particles, thereby strengthening conceptual understanding of both perspectives. The idea of particles arising as excitations of the fields naturally brings in the notion of Bogoliubov transformations. Using this, it is easy to understand the Unruh-Davies effect, viz., that the vacuum state in an inertial frame appears as a thermal state in a uniformly

accelerated frame. We next take up the detailed description of the quantization of the electromagnetic field. I do this first in the radiation gauge in order to get the physical results quickly and to explain the interaction of matter and radiation. This is followed by the covariant quantization of the gauge field which provides an opportunity to introduce the Fadeev-Popov technique in the simplest possible context, and to familiarize you with the issues that arise while quantizing a gauge field. Finally, I provide a detailed description of the Casimir effect which is used to introduce — among other things — the notion of dimensional regularization.

4. **Real Life I: Interactions.** Having described the free quantum fields, we now turn to the description of interacting fields. The standard procedure in textbooks is to introduce perturbation theory, obtain the Feynman rules, calculate physical processes, and then introduce renormalization as a procedure to tackle the divergences in the perturbation theory, etc. For the reasons I described in the Preface, I think it is better to start from a non-perturbative approach, through the concept of effective action. I will do this both for $\lambda\phi^4$ theory and for electromagnetic field coupled to a complex scalar field. In both the cases, one is led to the concept of renormalization group and that of running coupling constants. These, in turn, allow us to introduce the Wilsonian approach to QFT, which is probably the best language available to us today to understand QFT. The notion of effective action also leads to the Schwinger effect, viz., the production of charged particles by a strong electric field. This effect is non-analytic in the electromagnetic coupling constant, and hence cannot be obtained by perturbation theory. After having discussed the non-perturbative effects, I turn to the standard perturbation theory for the $\lambda\phi^4$ case and obtain the usual Feynman diagrams (using functional integral techniques) and describe how various processes are calculated. This allows us to connect up themes like the effective Lagrangian and the running coupling

constant from both perturbative and non-perturbative perspectives.

5. **Real Life II: Fermions and QED.** Upto this point, I have avoided fermions in order to describe the issues of QFT in a simplified setting. This last chapter is devoted to the description of fermions and, in particular, QED. The Dirac equation is introduced in a slightly novel way through the relativistic square root $\sqrt{p^2} = \gamma^a p_a$, after discussing the corresponding non-relativistic square root $\sqrt{p^2} = \boldsymbol{\sigma} \cdot \mathbf{p}$ and the Pauli equation. Having obtained the Dirac equation, I describe the standard lore related to Dirac matrices and obtain the magnetic moment of the electron. I then proceed to discuss the quantization of the Dirac field, paying careful attention to the role of causality in fermionic field quantization. The path integral approach to fermionic fields is introduced through Grassmannians (which is developed to the extent required) and once again, we will begin with non-perturbative features like the Schwinger effect for electrons, before discussing perturbation theory and the Feynman rules in QED. Finally, I provide a detailed discussion of the one loop QED and renormalization. This will allow, as an example, the computation of the anomalous magnetic moment of the electron, which many consider to be the greatest triumph of QED. The discussion of one loop diagrams in QED also allows the study of renormalization in the perturbative context and connect up the “running” of the electromagnetic coupling constant computed by the perturbative and non-perturbative techniques.